



Solution of missing GT strength problem and spin-dipole resonance

- ❖ Neutron measurement
- ❖ Proportionality between (p,n) 0° cross section and $B(GT)$
- ❖ Theoretical solutions for missing GT strength problem
- ❖ Multipole decomposition analysis
- ❖ Experimental solution for missing GT strength problem
- ❖ Sum rules for higher-multipole excitations
- ❖ Spin-dipole resonance
- ❖ Homework

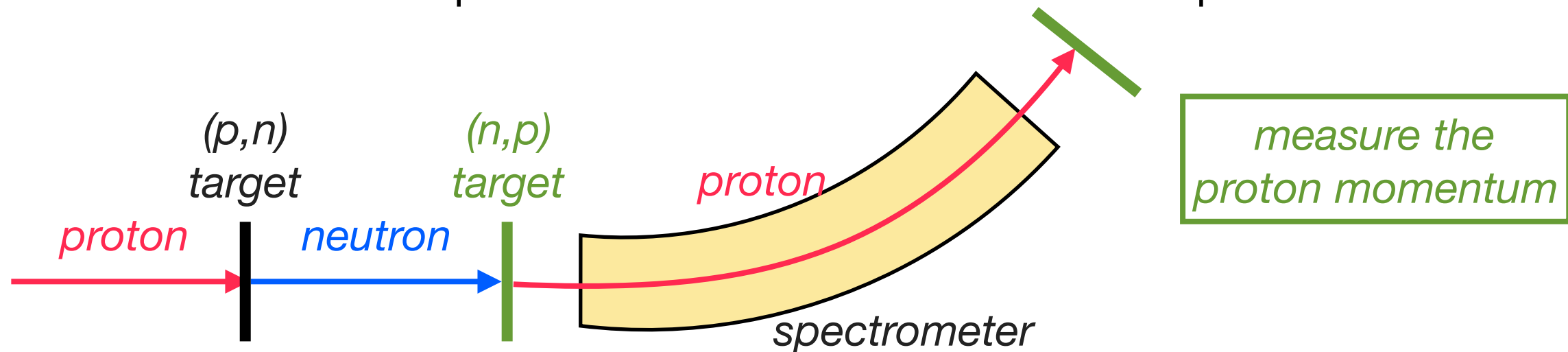
Neutron measurements

(p,n) reactions

Two different techniques for analyzing intermediate-energy neutron momentum:

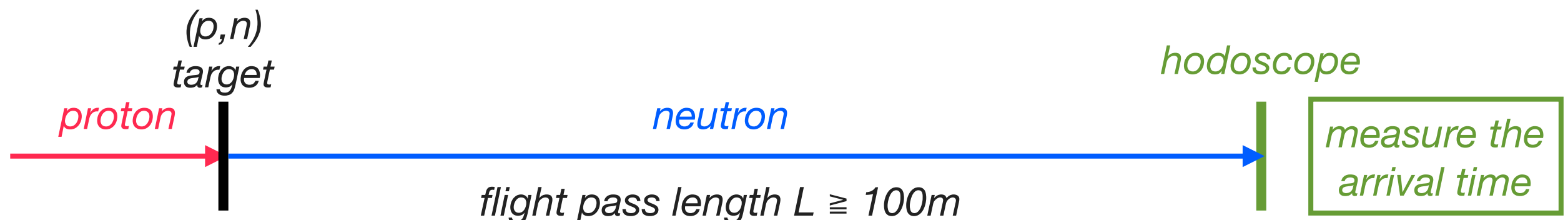
Charge-exchange method:

- Transfer the neutron momentum to a proton via a secondary (n,p) reaction.
- Measure the recoiled proton momentum in a conventional spectrometer.



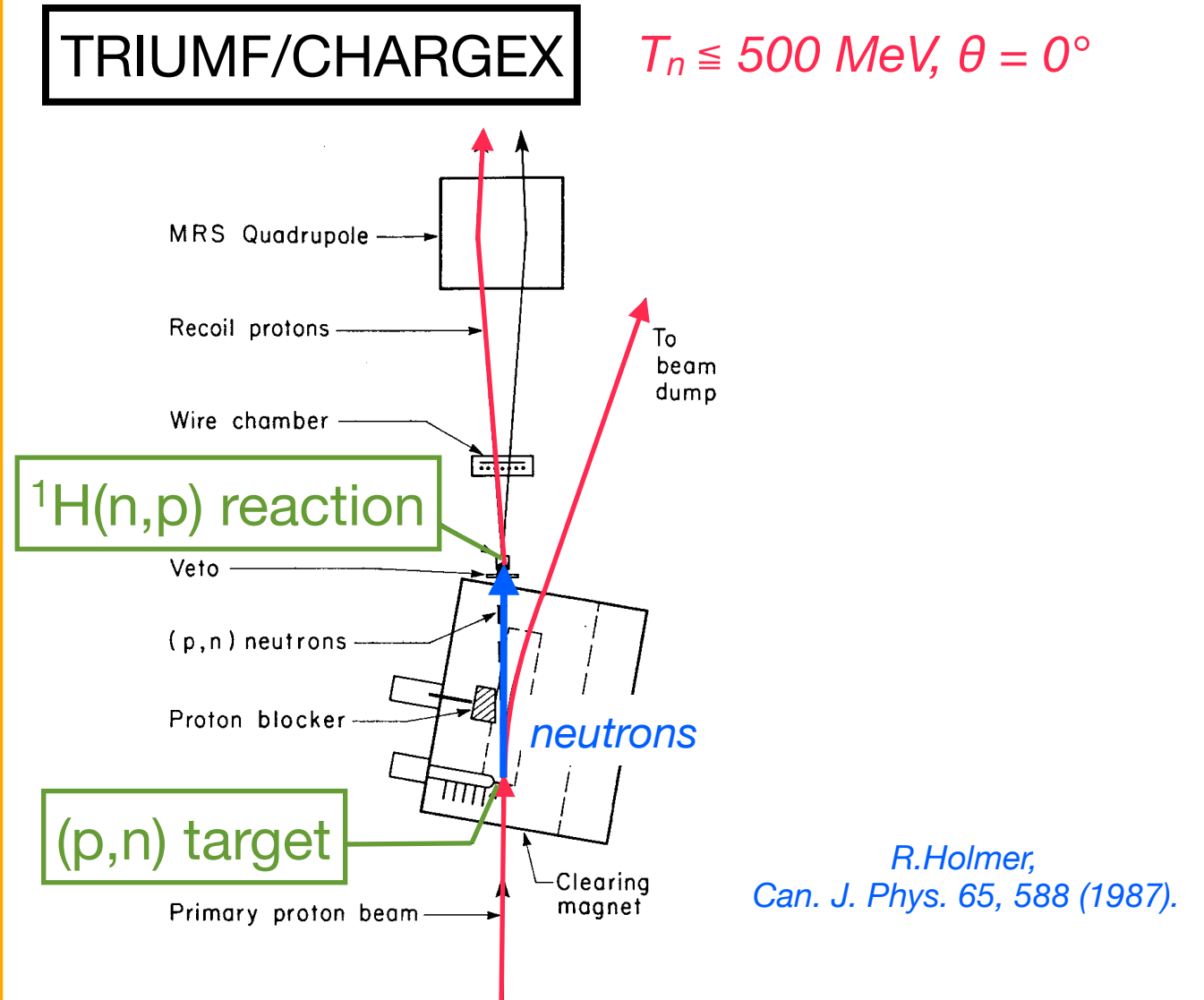
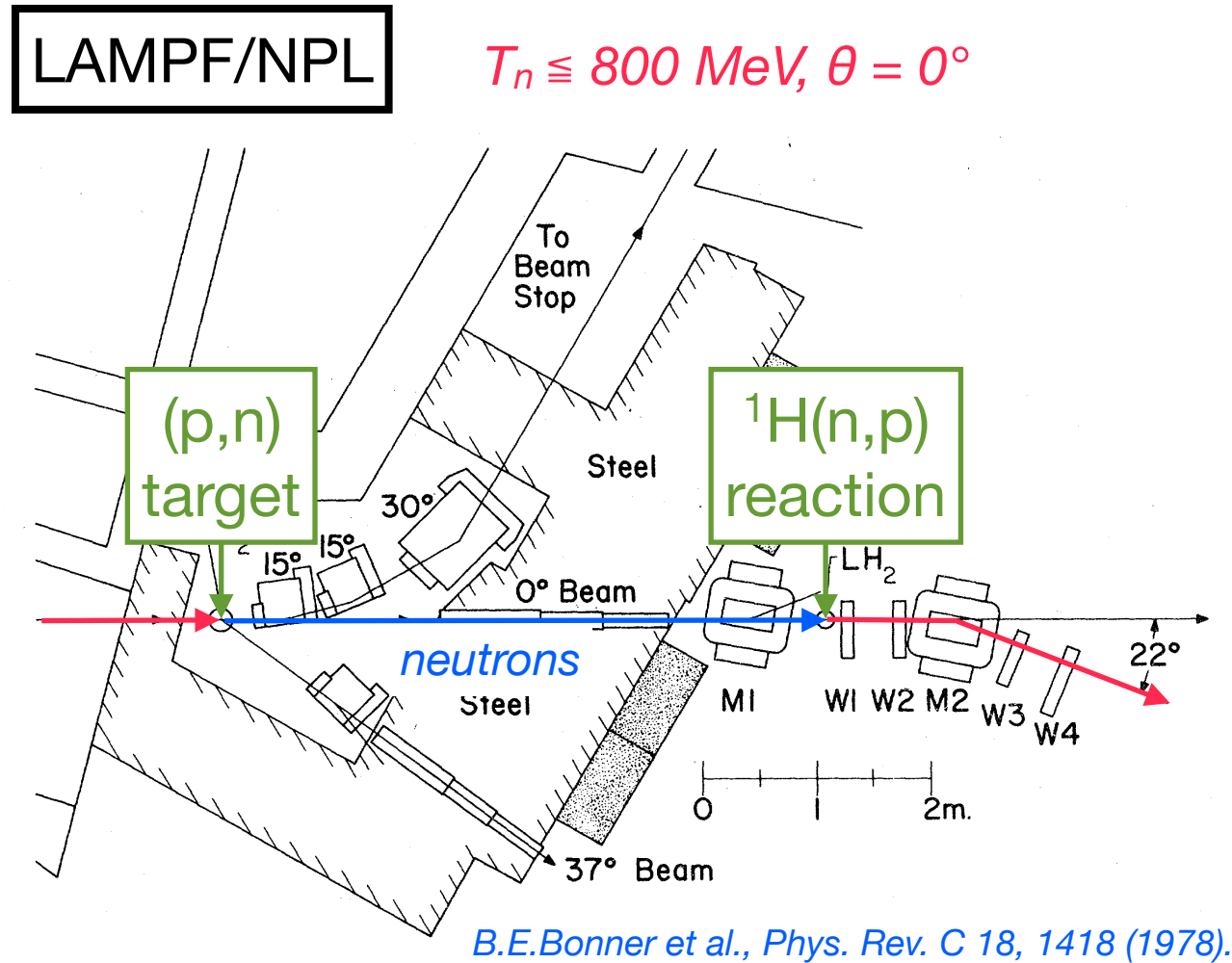
Time-Of-Flight (TOF) method:

- Measure the neutron TOF by detecting its arrival time at a hodoscope.
- Flight path length L is fixed and typically $L \geq 100$ m.



Neutron charge-exchange facilities

Neutrons are converted to protons by $^1\text{H}(n,p)$ and protons are analyzed/measured.



Advantage:

- Enable (p,n) studies where long TOF paths are not feasible.

Disadvantage:

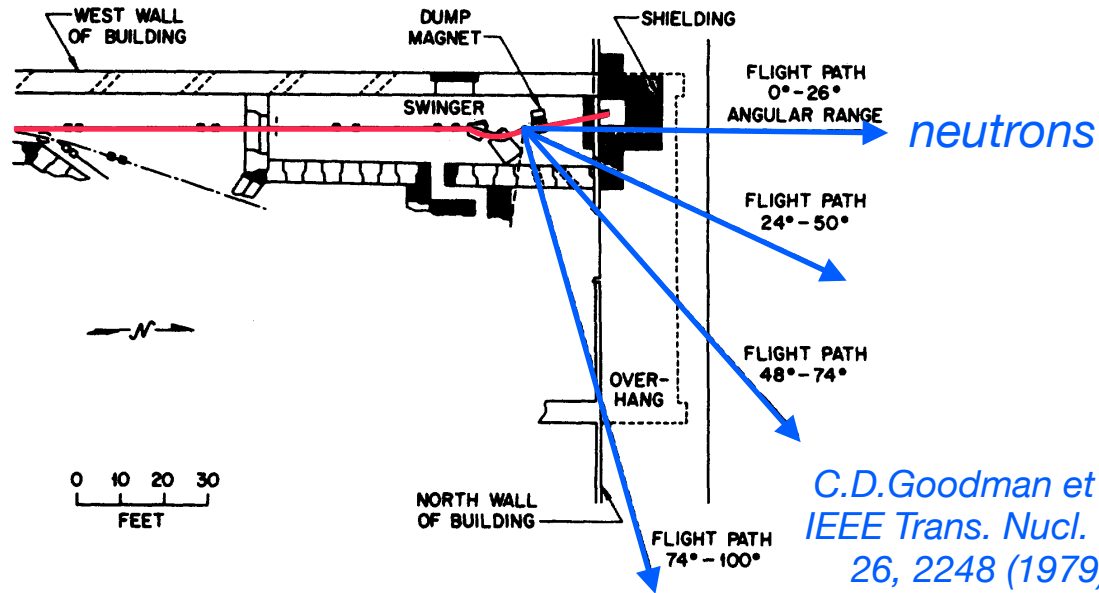
- Final energy resolutions are limited to about 1 MeV.
- Difficult to measure polarization transfers.

can overcome by TOF method

Neutron TOF facilities

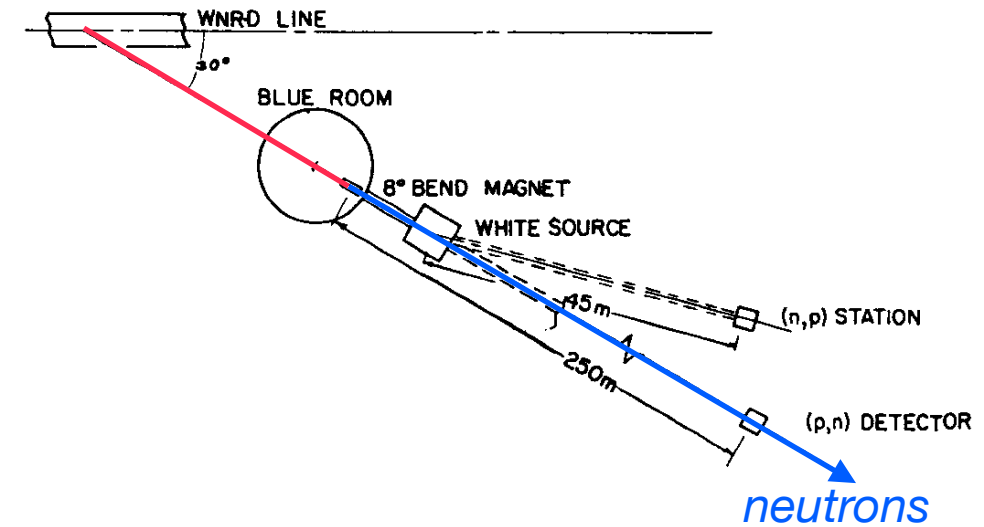
Neutron energies are determined by measuring their time-of-flight (TOF).

IUCF $T_n = 50\text{-}200\text{ MeV}$, $L_{TOF} = 100\text{ m}$, $\theta = 0^\circ\text{-}100^\circ$



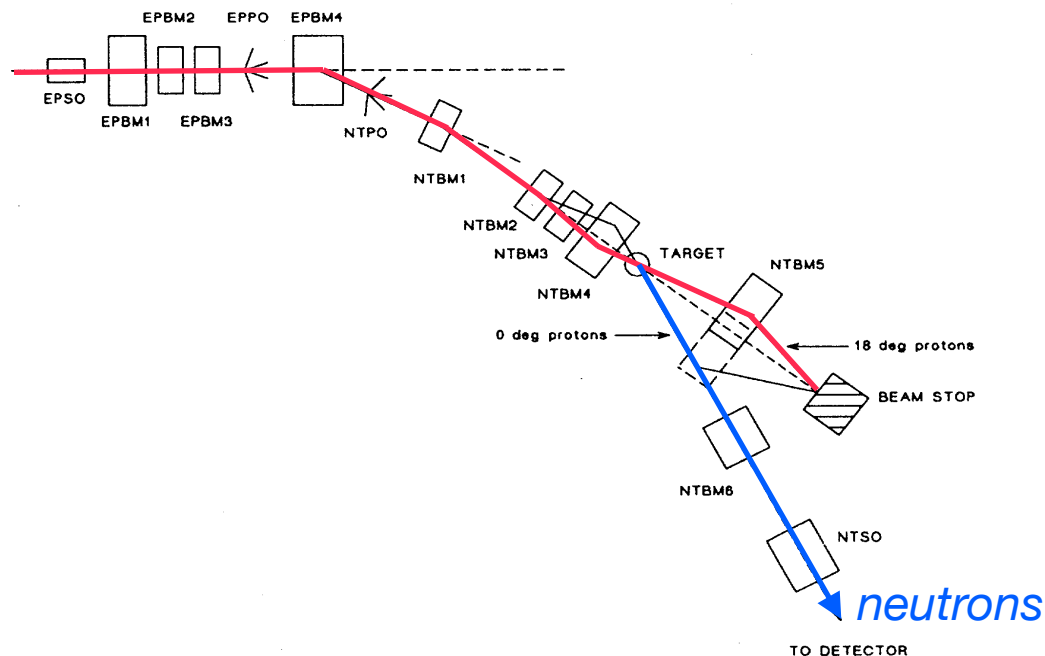
C.D. Goodman et al.,
IEEE Trans. Nucl. Sci.
26, 2248 (1979).

LAMPF/WNR $T_n \leq 800\text{ MeV}$, $L_{TOF} = 250\text{ m}$, $\theta = 0^\circ\text{-}9^\circ$



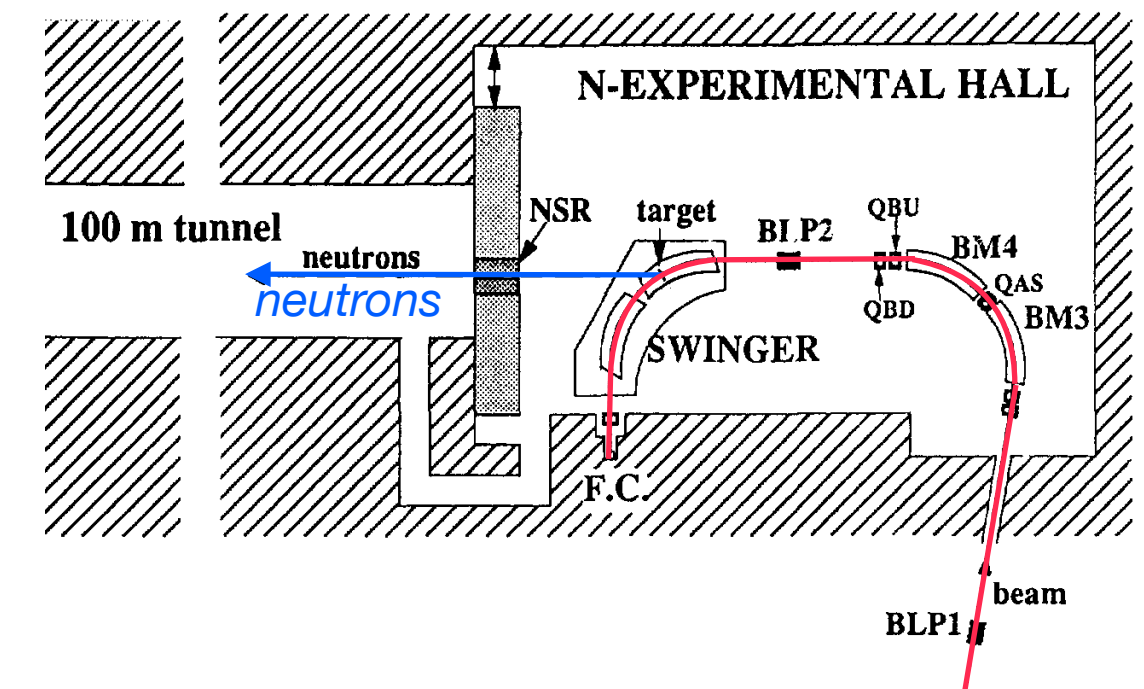
D.A. Lind,
Can. J. Phys.
65, 637 (1987).

LAMPF/NTOF $T_n \leq 800\text{ MeV}$, $L_{TOF} \leq 620\text{ m}$, $\theta \leq 27^\circ$



X.Y.Chen et al., Phys. Rev. C 47, 2159 (1993).

RCNP/NTOF $T_n \leq 400\text{ MeV}$, $L_{TOF} \leq 100\text{ m}$, $\theta \leq 40^\circ$

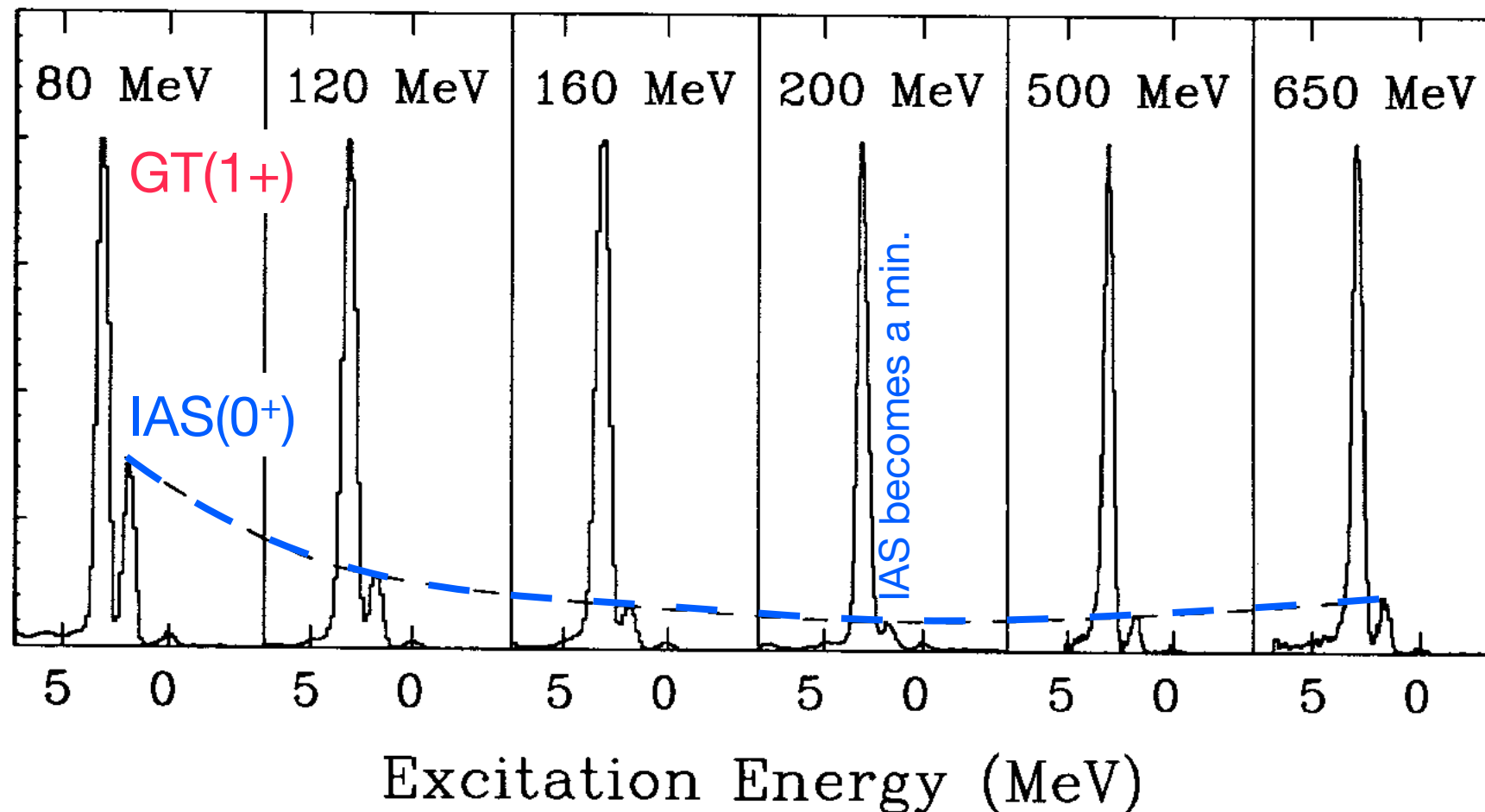


H.Sakai et al., Nucl. Instrum. Methods 369, 120 (1996).

TOF spectra and Neutron detection efficiency

J.Rapaport and E.Sugarbaker, Ann. Rev. Nucl. Part. Sci. 44, 109 (1994).

Typical TOF energy spectra for $^{14}\text{C}(p,n)^{14}\text{N}$ at 80-650 MeV and 0 degrees



Good energy resolutions

- 200 keV at $T_n \leq 200$ MeV
- 650 keV at $T_n = 650$ MeV

Note: Other typical (p,n) spectra for light, medium, and heavy nuclei are given in Appendix A.

Detection of fast neutrons with good energy resolutions:

- Accomplished with relatively small detector volume (for good timing resolution in TOF).
- Detection efficiency $\varepsilon < 100\%$

Efficiency ε should be determined to derive cross sections:

Exercise/Homework:

Explain how the neutron detector's efficiency is determined by referring Appendix B.

Proportionality between (p,n) cross section and B(GT)

Empirical proportionality between (p,n) $\sigma(0^\circ)$ and B(GT)

For low-lying GT states, following two values were measured.

- Beta decay transition strengths : B(GT)
- Cross sections by (p,n) at 0° ($q \sim 0$)

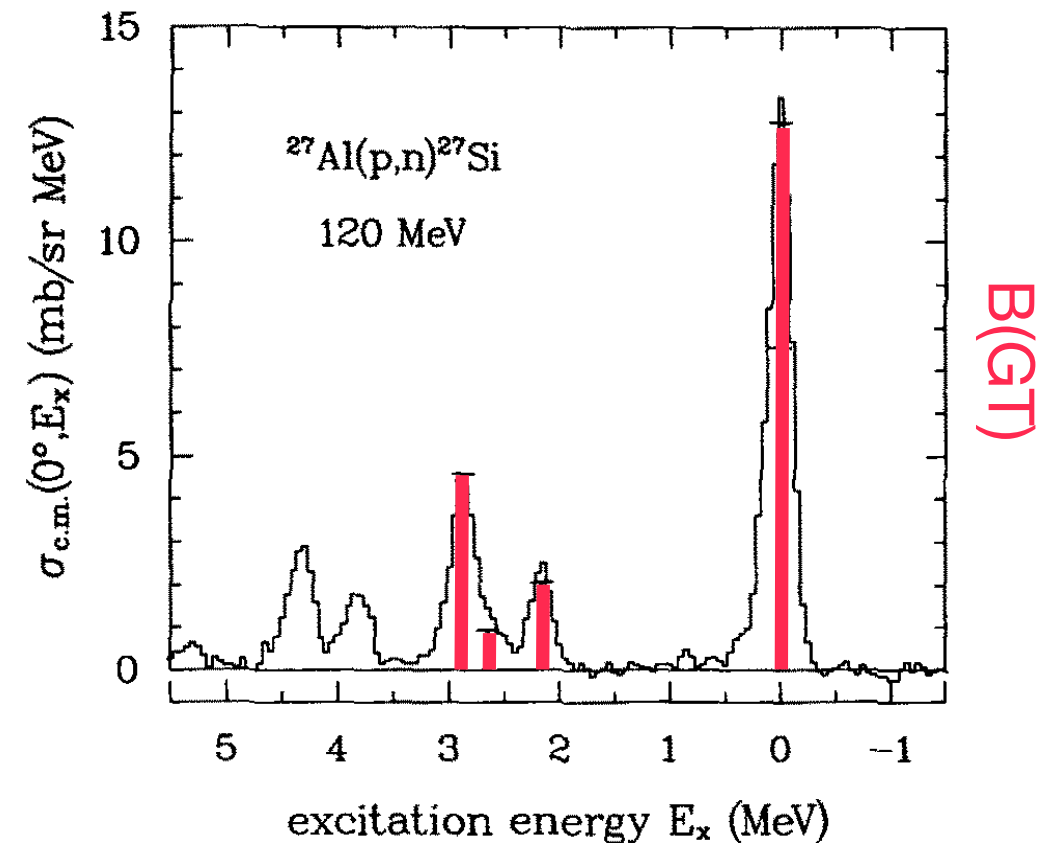
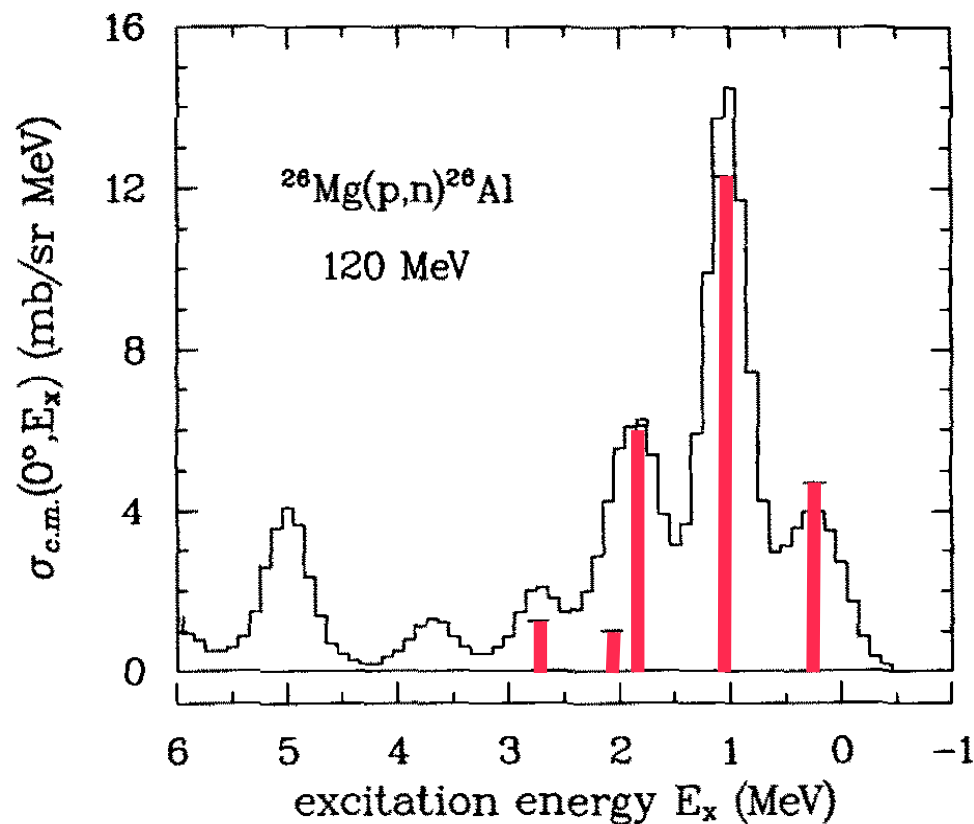
Empirical proportionality has been found/established.

$$\sigma(0^\circ) = \hat{\sigma}_{\text{GT}}(A) F(q, \omega) B(\text{GT}) \simeq \hat{\sigma}_{\text{GT}}(A) B(\text{GT})$$

- $\hat{\sigma}_{\text{GT}}(A)$: GT unit cross section (proportionality coefficient)
A-dependent (and T_p -dependent)
- $F(q, \omega)$: (q, ω) correction factor ($F(0,0)=1$)

Ref.
Lecture by Ichimura-san
“PWBA”

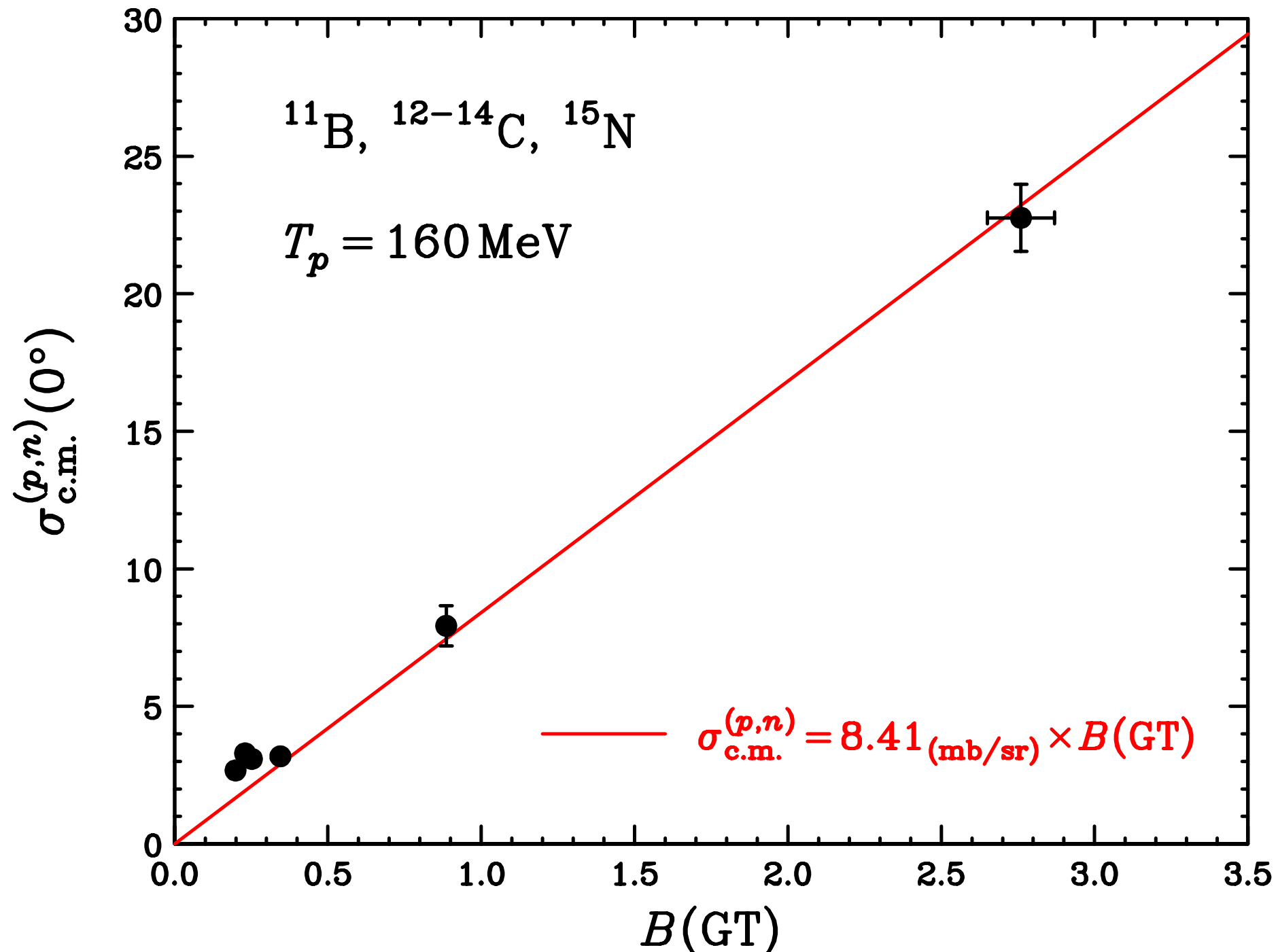
*T.N. Taddeucci et al.,
Nucl. Phys. A 469, 125 (1987).*



Proportionality between (p,n) $\sigma(0^\circ)$ and B(GT)

Experimental results for the GT transitions in p-shell nuclei

Proportionality between (p,n) $\sigma(0^\circ)$ and B(GT) has been established.

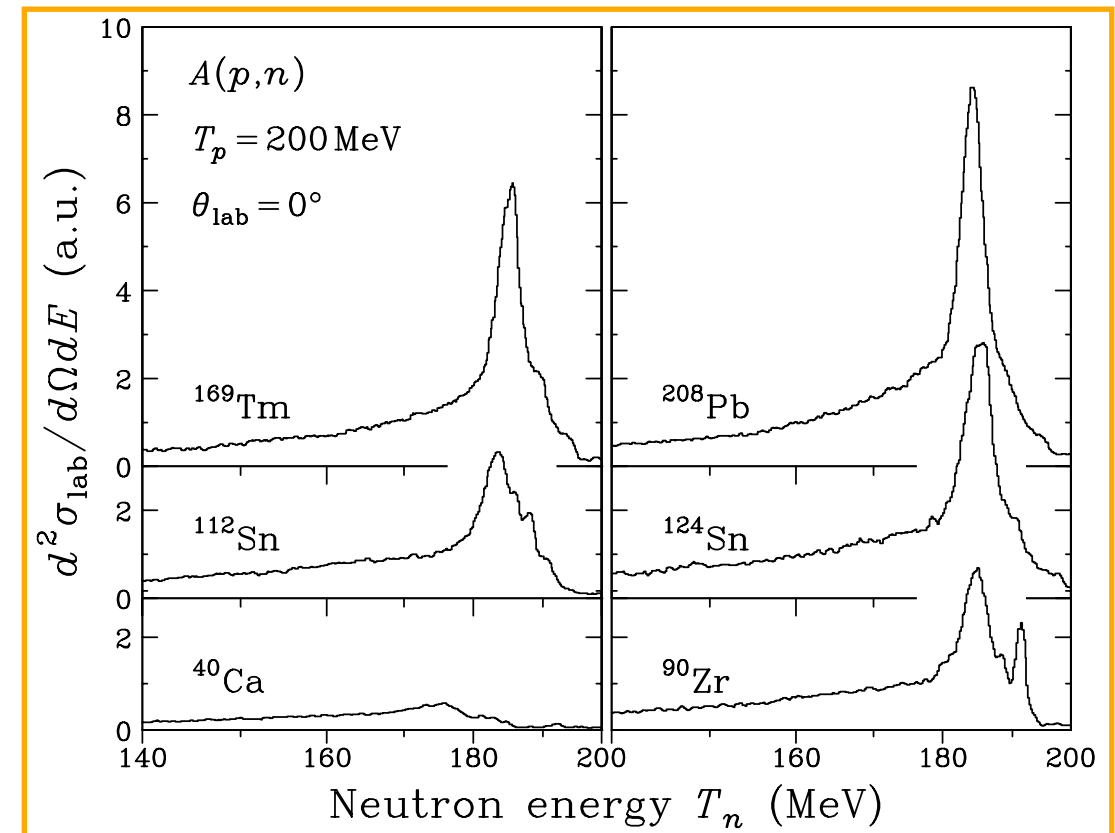


Missing GT strength problem

Experimental verification of GT sum rule

Experimental (p,n) cross section up to GTR is converted to B(GT)

- $\sigma^{(p,n)}(0^\circ) \simeq \hat{\sigma}_{GT}(A) \cdot B(GT)$
- Beyond GTR, $L \geq 1$ excitations would be dominant \rightarrow excluded.

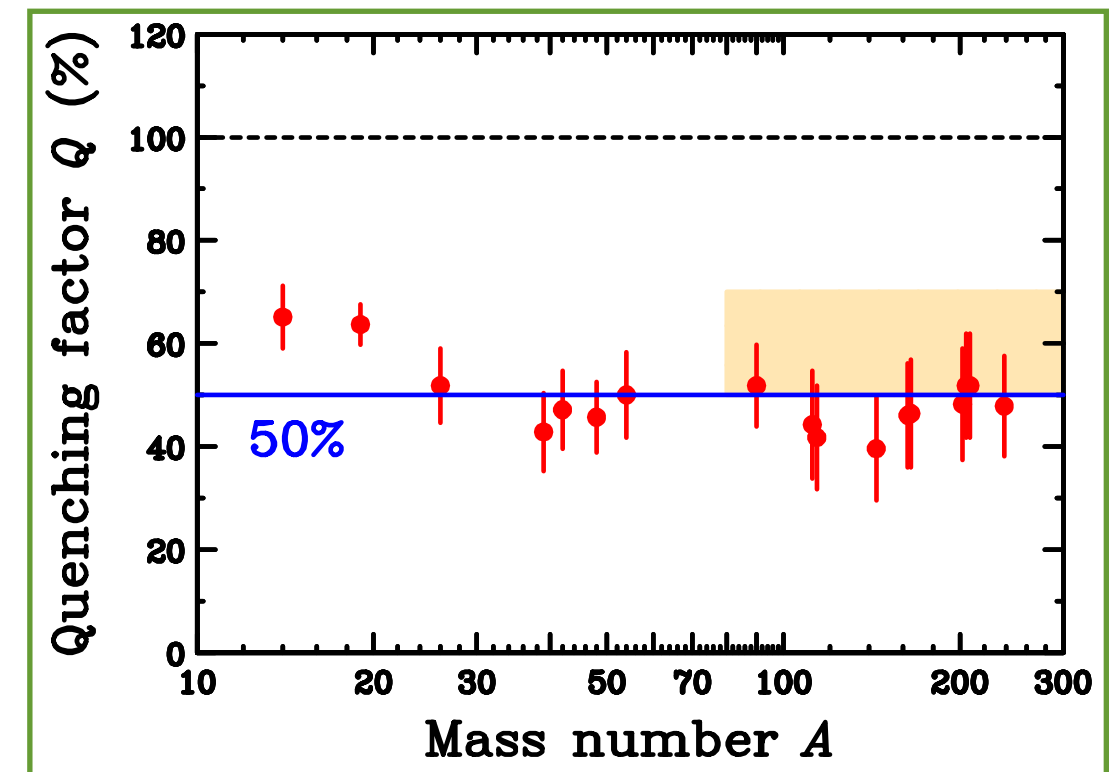


Fraction of GT sum-rule strength

Experimental $S(GT_-) = 50-60\%$ of $3(N-Z)$

- $3(N-Z)$ is the minimum value in the case of $S(GT_+) = 0$.

\rightarrow missing GT strength problem



Theoretical solutions for the “missing GT strength” problem

Two possible mechanisms for GT quenching effect

Quark-degree (Δ -isobar) effect

A nucleon is assumed as a bag of three quarks.

GT $\Delta S = \Delta T = 1$ transition can excite nucleon (N) to Δ -isobar (Δ).

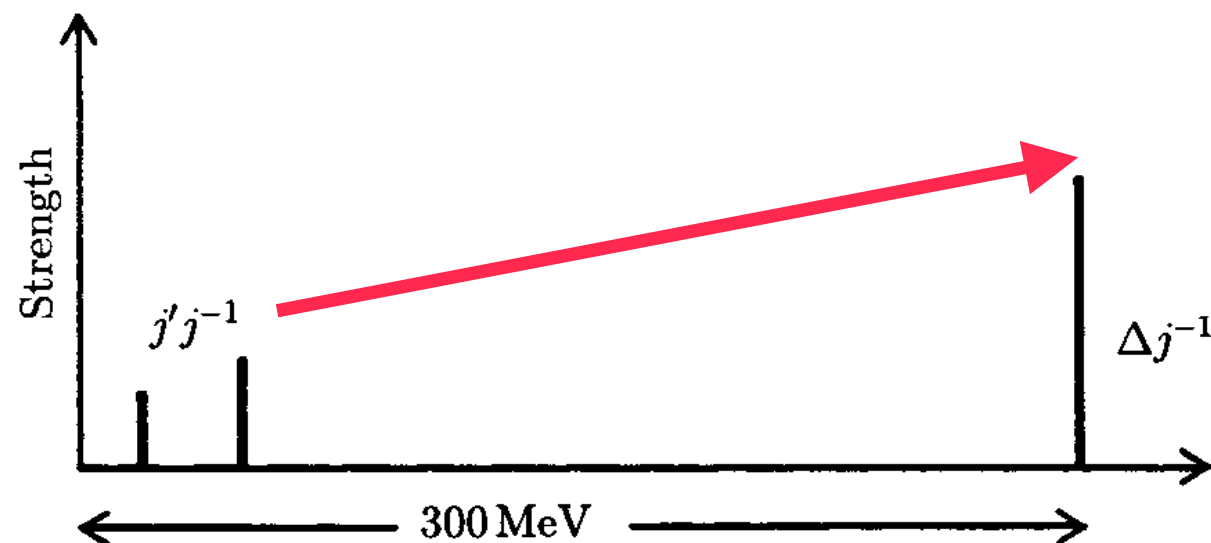


If the coupling between p-h and Δ -h is strong

- p-h excitations of GTR in $\omega \sim 10$ MeV mixed with Δ -h excitations at $\omega \sim 300$ MeV

Coupling is repulsive.

- GTR strength is moved to Δ -h excitation region \rightarrow GTR strength is quenched.



- no Pauli blocking for Δ excitation
- large number of Δ -h configurations

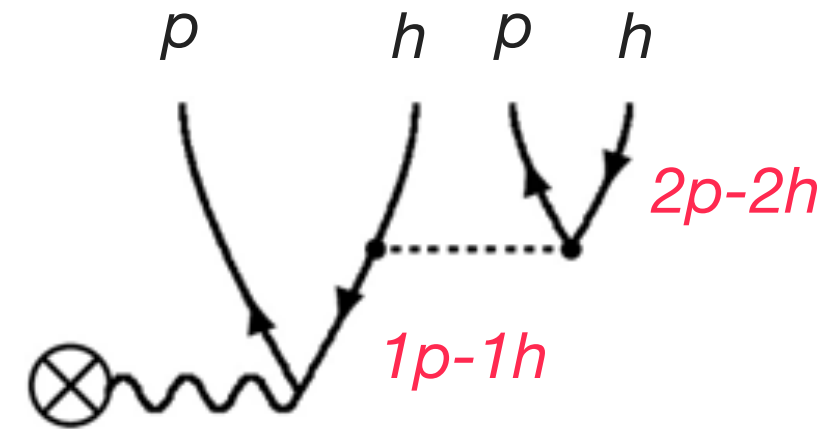
↓
able to bridge $\Delta\omega = 300$ MeV

Two possible mechanisms for GT quenching effect

Configuration mixing effect

1p-1h excitations mix with 2p-2h excitations

- GTR strength is moved to the continuum beyond GTR.



Theoretical prediction for $B(GT)$ of $^{90}\text{Zr}(p,n)$

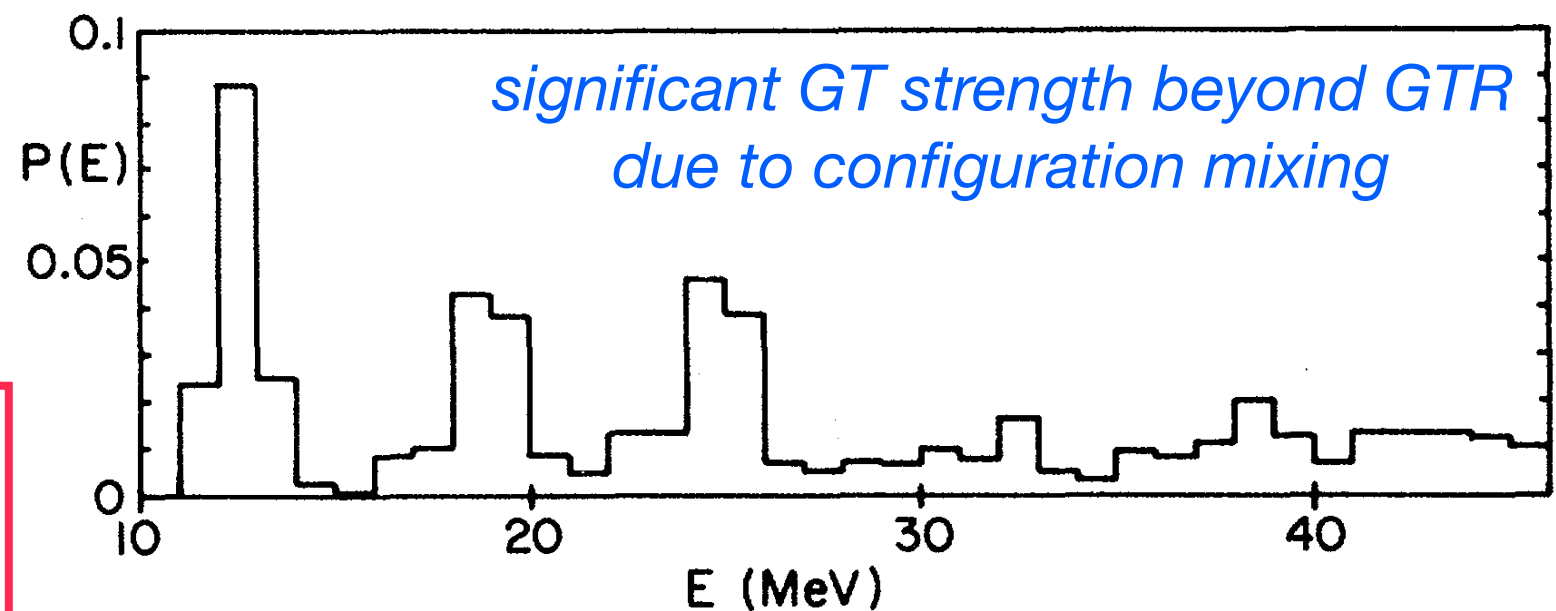
GTR < 10 MeV (NOT shown)

- $\sim 50\%$ of sum-rule

Coupling to 2p-2h configurations

- $\sim 50\%$ of sum-rule

*GTR is quenched by $\sim 50\%$
due to configuration mixing*



G.F.Bertsch and I.Hamamoto, Phys. Rev. C 26, 1323 (1982).

Separation/identification of $B(GT)$ in continuum ($\omega > 20$ MeV) is important.

The “extended” Landau-Migdal interaction

The “original” Landau-Migdal interaction V_{LM} is:

$$V_{LM} = C_0 [f_0 + f'_0(\tau_1 \cdot \tau_2) + g_0(\sigma_1 \cdot \sigma_2) + g'_0(\sigma_1 \cdot \sigma_2)(\tau_1 \cdot \tau_2)]$$

- V^{LM} is a zero-range interaction

For GT ($\Delta S = \Delta T = 1$) excitation, the following spin-isospin term contributes:

spin-isospin ($\Delta S = \Delta T = 1$) : $V_{LM}^{\sigma\tau} = C_0 g'(\tau_1 \cdot \tau_2)(\sigma_1 \cdot \sigma_2)$ we set $g'_0 \equiv g'$

- pionic unit : $C_0 = \frac{f_{\pi NN}^2}{m_\pi^2} \simeq 400 \text{ MeV fm}^3$

The Landau-Migdal interaction can be extended to include Δ as:

$$V_{LM} = \left[\underbrace{\frac{f_{\pi NN}^2}{m_\pi^2} g'_{NN}}_{\text{coupling b/w p-h states}} + \underbrace{\frac{f_{\pi NN} f_{\pi N\Delta}}{m_\pi^2} g'_{N\Delta}}_{\text{coupling b/w p-h and } \Delta\text{-h states}} \right] (\tau_1 \cdot \tau_2)(\sigma_1 \cdot \sigma_2)$$

coupling b/w
p-h states

coupling b/w
p-h and Δ -h states

$f_{\pi NN}$: πNN coupling const.

$f_{\pi N\Delta}$: $\pi N\Delta$ coupling const.

Two Landau-Migdal parameters, g'_{NN} and $g'_{N\Delta}$

Two possible mechanisms and LM parameters

Landau-Migdal interaction with N and Δ :
$$V_{\text{LM}} = \frac{f_{\pi NN}^2}{m_\pi^2} g'_{NN} + \frac{f_{\pi NN} f_{\pi N\Delta}}{m_\pi^2} g'_{N\Delta}$$

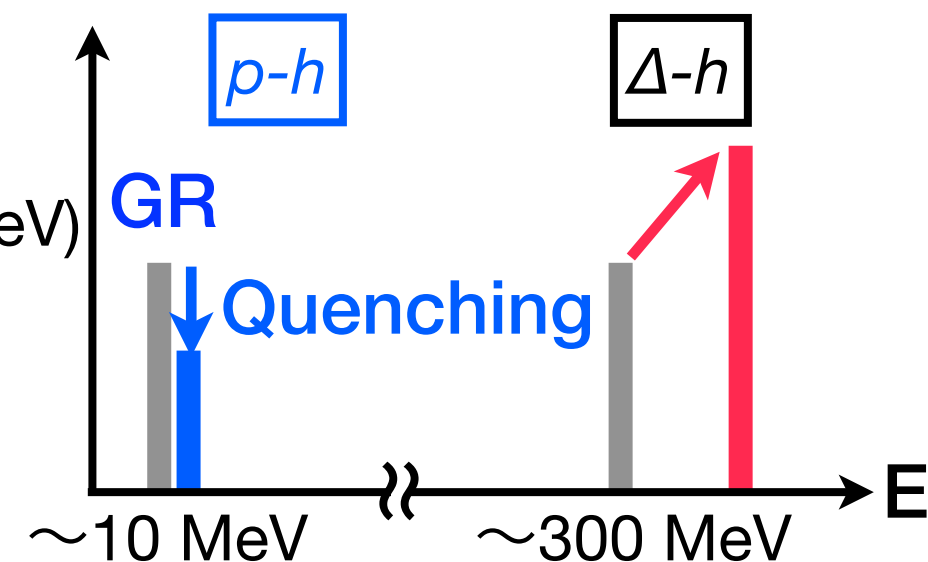
Quark-degree (Δ -isobar) effect

Assumption: $g'_{N\Delta} = g'_{NN}$ (universality ansatz)

Coupling between p-h and Δ -h is *large (strong repulsion)*

- Significant GT strengths move to Δ region ($\omega \sim 300$ MeV)
- GTR strength is quenched

Strength



Configuration mixing effect

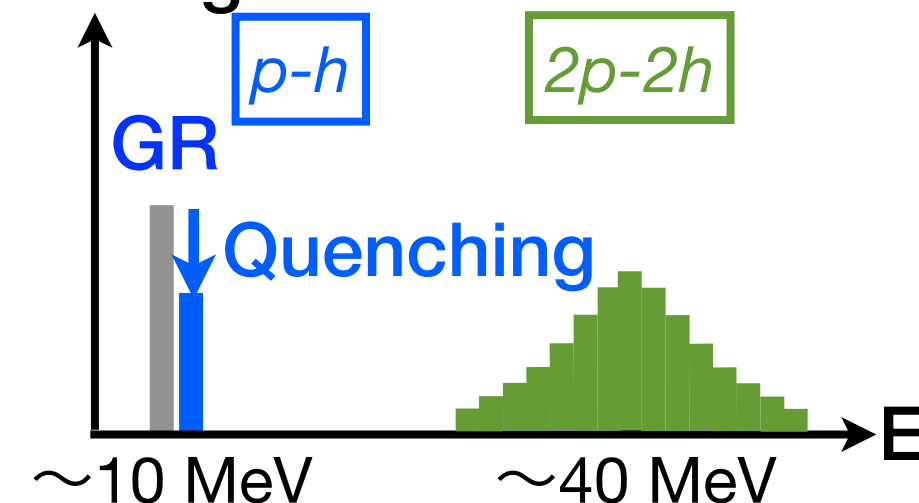
In microscopic calculations, $g'_{N\Delta} < g'_{NN}$ [$g'_{N\Delta} \simeq (0.6 - 0.7)g'_{NN}$]

- One-boson ex. model by Arima et al., and Towner et al.
- G-matrix calc. by Dickhoff et al. and Nakayama et al.

Coupling between p-h and Δ -h is *small (weak repulsion)*

- Strength-shift to Δ region is small
- GTR strength is quenched by configuration mixing

Strength



g'_{NN} and $g'_{N\Delta}$ dependences on GTR

T.W. et al., Phys. Rev. C 72, 067303 (2005).

Landau-Migdal interaction at $q=0$

$$V_{LM} = \frac{f_{\pi NN}^2}{m_\pi^2} \underbrace{g'_{NN}}_{\substack{\text{repulsion between} \\ \text{particle and hole (ph)}}} + \frac{f_{\pi NN} f_{\pi N\Delta}}{m_\pi^2} \underbrace{g'_{N\Delta}}_{\substack{\text{coupling between} \\ \text{ph and } \Delta h}}$$

LM parameter g'_{NN}

Determine the p-h repulsion

Larger $g'_{NN} \rightarrow$ Stronger repulsion

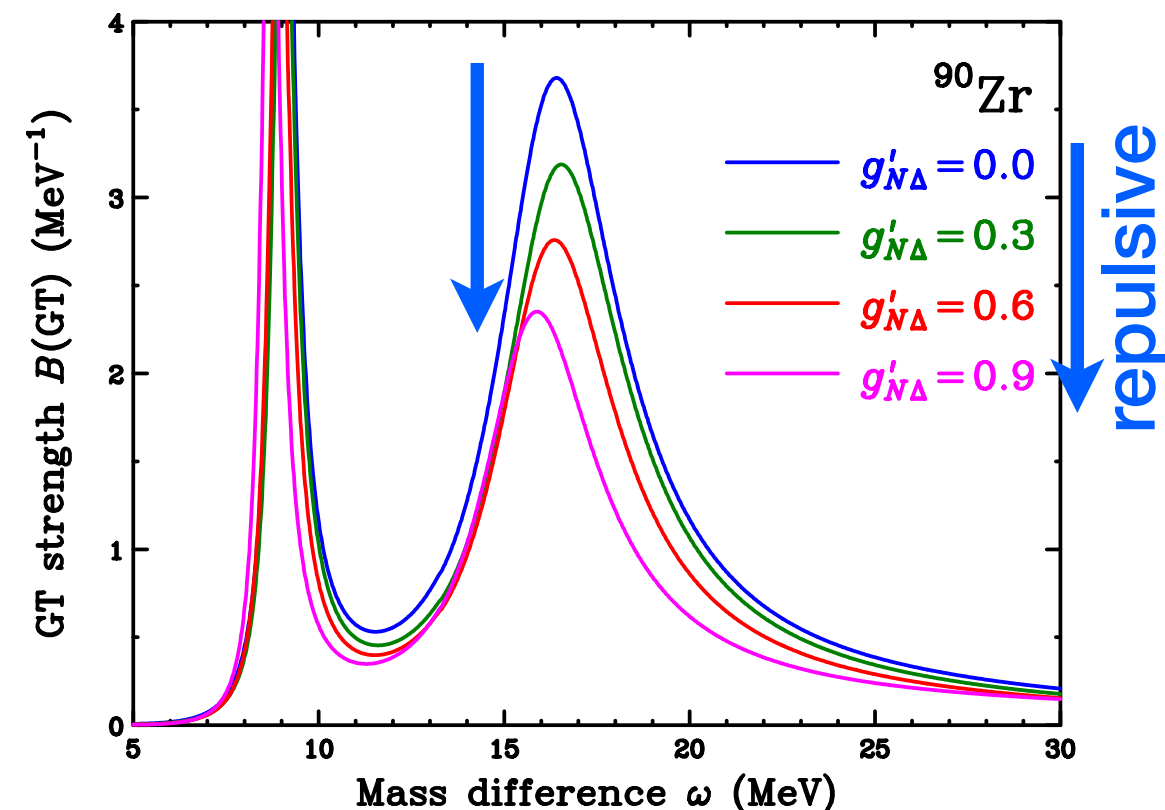
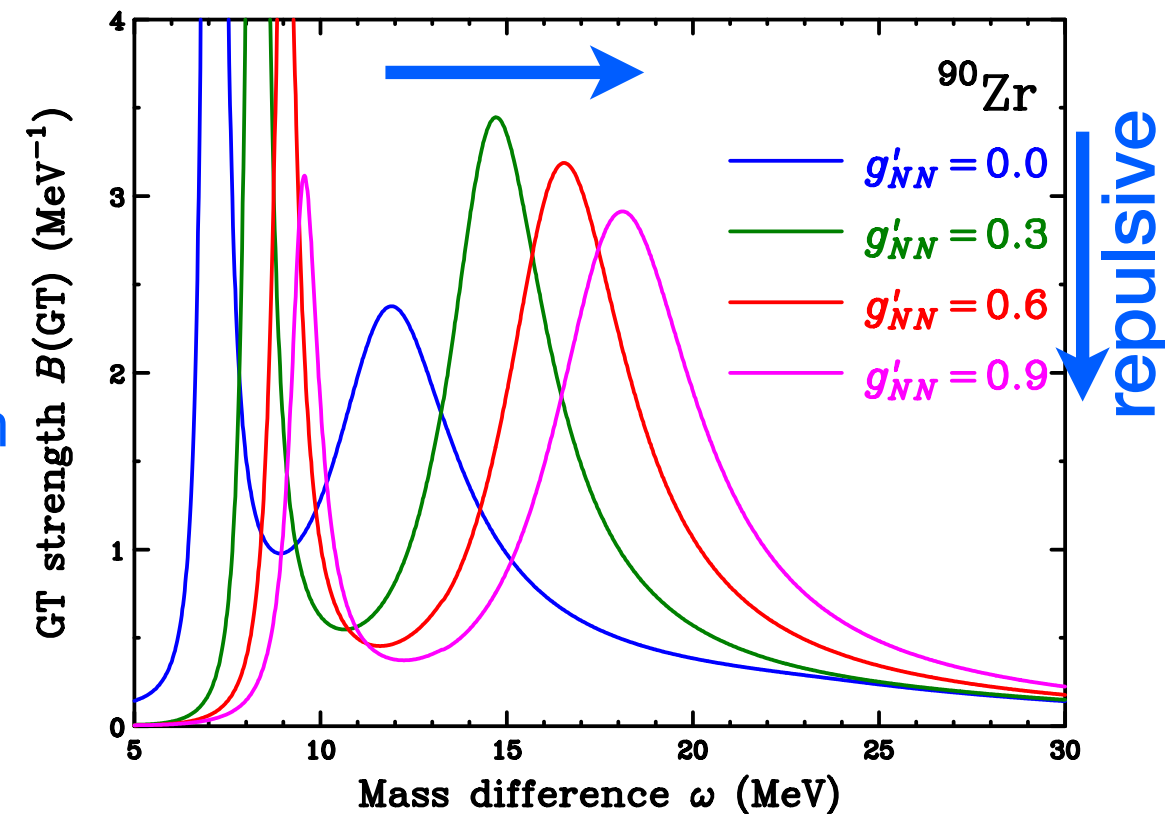
- Peak shifts to higher ω
- Collectivity becomes large

LM parameter $g'_{N\Delta}$

Determine the coupling to Δ

Larger $g'_{N\Delta} \rightarrow$ Stronger coupling

- Strength becomes small (quenched)
[Strength moves to Δ region]



Multipole decomposition analysis

How to extract the GT strength in the continuum

There would be GT $\Delta L=0$ strength:

- below the GTR
- beyond the GTR

Extraction of these GT strength in the continuum:

Assumption:

- The measured cross section at an energy transfer ω is a coherent sum of cross sections from several ΔL

$$\sigma(\omega) = \sum_{\Delta L} a_{\Delta L} \sigma_{\Delta L}(\omega) = a_{\Delta L=0} \sigma_{\Delta L=0}(\omega) + a_{\Delta L=1} \sigma_{\Delta L=1}(\omega) + \dots$$

- $a_{\Delta L}$: relative strengths of the individual multipoles

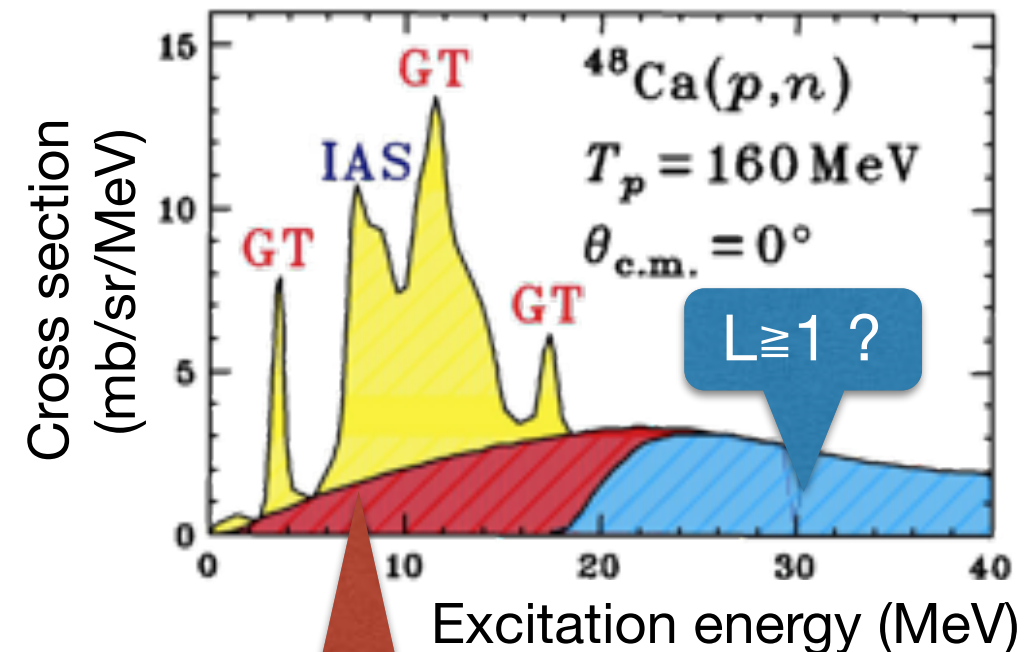
Note:

- In practice, $\sigma(\omega)$ is expressed as an incoherent sum of c.s. from several ΔJ^π as

$$\sigma(\omega) = \sum_{\Delta J^\pi} a_{\Delta J^\pi} \sigma_{\Delta J^\pi}(\omega)$$

- In general, the possible three $\Delta J = \Delta L \pm 1, \Delta L$ members for a ΔL are grouped because of the small ΔJ dependence.

Here, we express $\sigma(\omega)$ as a incoherent sum of cross sections from several ΔL for simplicity.



B.G. or GT ?

$L \geq 1 ?$

How to extract the GT strength in the continuum

Assumption:

$$\sigma(\omega) = \sum_{\Delta L} a_{\Delta L} \sigma_{\Delta L}(\omega) = a_{\Delta L=0} \sigma_{\Delta L=0}(\omega) + a_{\Delta L=1} \sigma_{\Delta L=1}(\omega) + \dots$$

Because $a_{\Delta L}$ should be independent of angle θ , angle dependence can be expressed as

$$\begin{array}{l} \sigma(\theta_1, \omega) \\ \sigma(\theta_2, \omega) \\ \sigma(\theta_3, \omega) \\ \vdots \end{array} = \begin{array}{l} a_{\Delta L=0} \sigma_{\Delta L=0}(\theta_1, \omega) \\ a_{\Delta L=0} \sigma_{\Delta L=0}(\theta_2, \omega) \\ a_{\Delta L=0} \sigma_{\Delta L=0}(\theta_3, \omega) \\ \vdots \end{array} + \begin{array}{l} a_{\Delta L=1} \sigma_{\Delta L=1}(\theta_1, \omega) \\ a_{\Delta L=1} \sigma_{\Delta L=1}(\theta_2, \omega) \\ a_{\Delta L=1} \sigma_{\Delta L=1}(\theta_3, \omega) \\ \vdots \end{array} + \dots$$

experimental data *angular-distribution of $\Delta L=0$ cross section* *angular-distribution of $\Delta L=1$ cross section*

If angular distributions (θ -dependences) of $\sigma_{\Delta L=0}$ and $\sigma_{\Delta L=1}$ are significantly different, relative strengths $a_{\Delta L}$ can be determined by a χ^2 fitting.

ΔL dependence on cross section

The (p,n) reaction mainly occurs around the nuclear surface (\because strong absorption)

The angular momentum transfer, ΔL , is related to momentum transfer, q , and nuclear radius, R , as

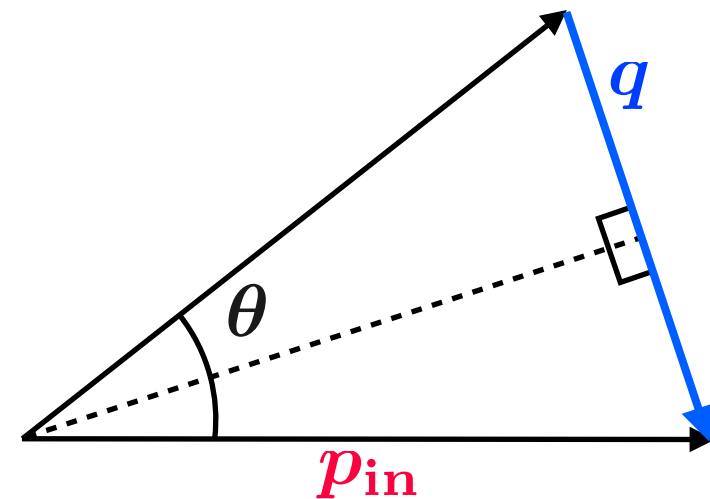
$$\Delta L \simeq q \cdot R \quad \dots \textcircled{1}$$

The momentum transfer q is expressed with the incident momentum p_{in} and scattering angle θ as:

$$q \simeq 2p_{\text{in}} \sin \frac{\theta}{2} \quad \dots \textcircled{2}$$

From $\textcircled{1}$ and $\textcircled{2}$, we get

$$\Delta L \simeq 2p_{\text{in}} R \sin \frac{\theta}{2}$$



Thus, the cross section takes a maximum at θ depending on ΔL .

Expectations for $^{208}\text{Pb}(p,n)$ at 200 MeV

- $p_{\text{in}} = 640 \text{ MeV}/c$
- $R \simeq 1.1A^{1/3} \times 80\% \simeq 5 \text{ fm}$

Angular distributions would be strongly depend on ΔL

| $^{208}\text{Pb}(p,n)$ | θ |
|------------------------|-----------|
| $\Delta L=0$ | 0° |
| $\Delta L=1$ | 4° |
| $\Delta L=2$ | 8° |

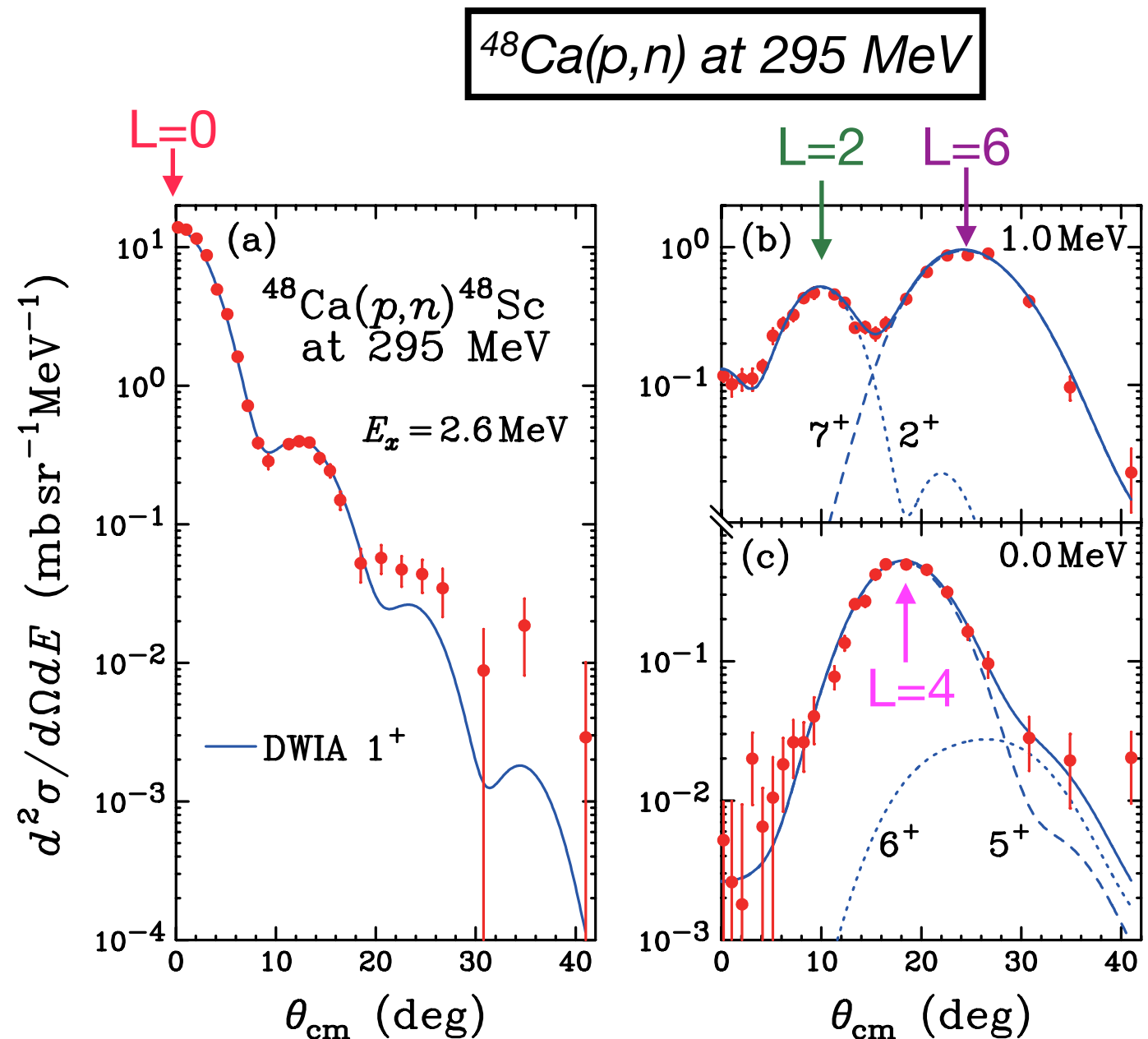
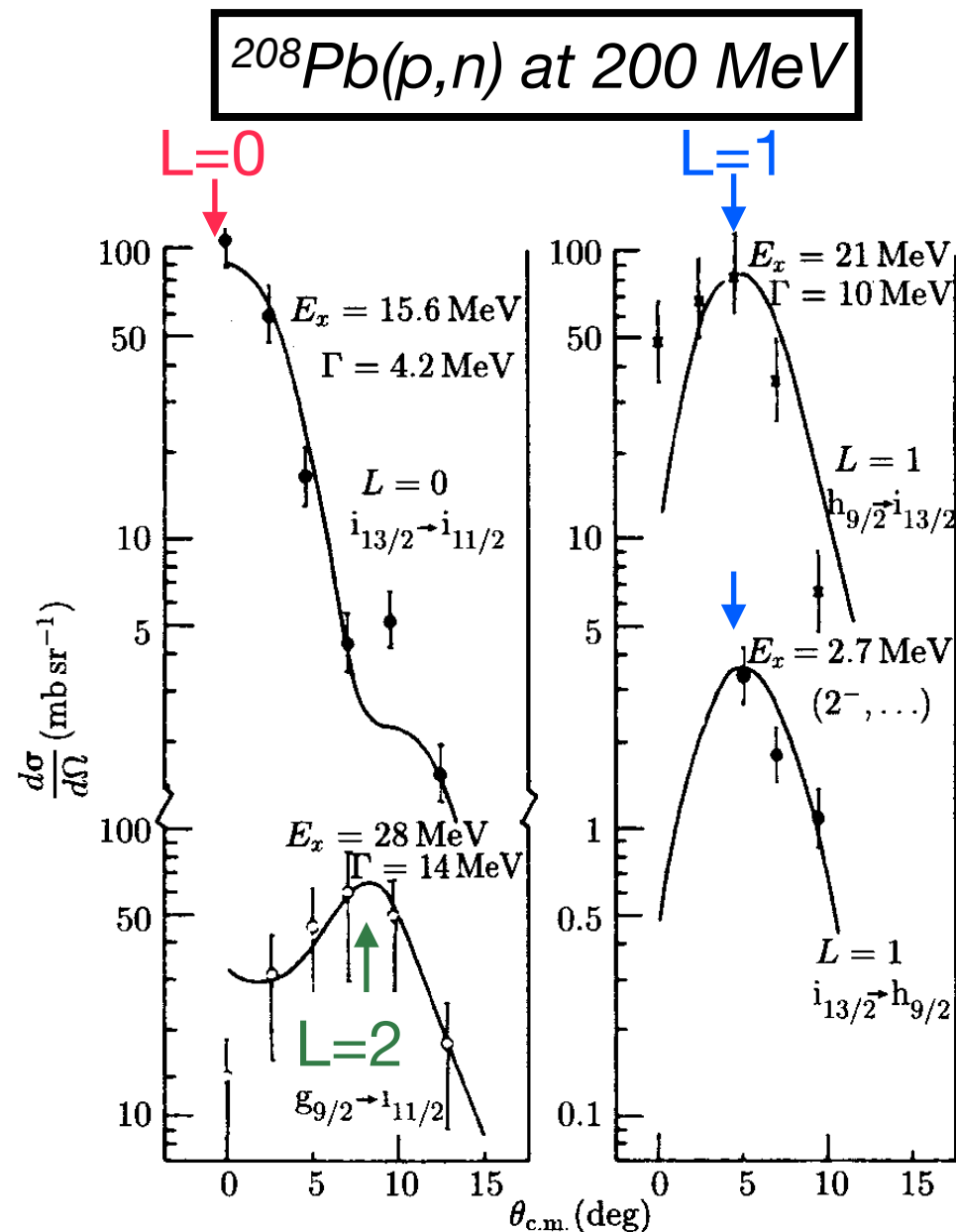
Angular distributions in DWIA

Comparison between experimental angular distributions and DWIA calculations.

Angular distributions are characterized by angular momentum transfer ΔL .

- Peak positions shift to larger angles w/ increasing ΔL *as expected*.

Experimental angular distributions are *well reproduced by DWIA calculations*.



Multipole decomposition analysis

K.Yako et al., Phys. Lett. B 615, 193 (2005).

M.Ichimura, H.Sakai, T.W., Prog. Part. Nucl. Phys. 56, 446 (2006).

For each energy transfer ω , it is assumed that:

The measured c.s. = An incoherent sum of c.s. arising from different ΔJ^π

$$\sigma^{\text{exp}}(\theta, \omega) = \sum_{\Delta J^\pi} a_{\Delta J^\pi} \sigma_{\Delta J^\pi}^{\text{calc}}(\theta, \omega)$$

- $a_{\Delta J^\pi}$: relative strengths of the individual multipoles
- $\sigma_{\Delta J^\pi}^{\text{calc}}$: angular distributions obtained by DWIA calculations

Data:

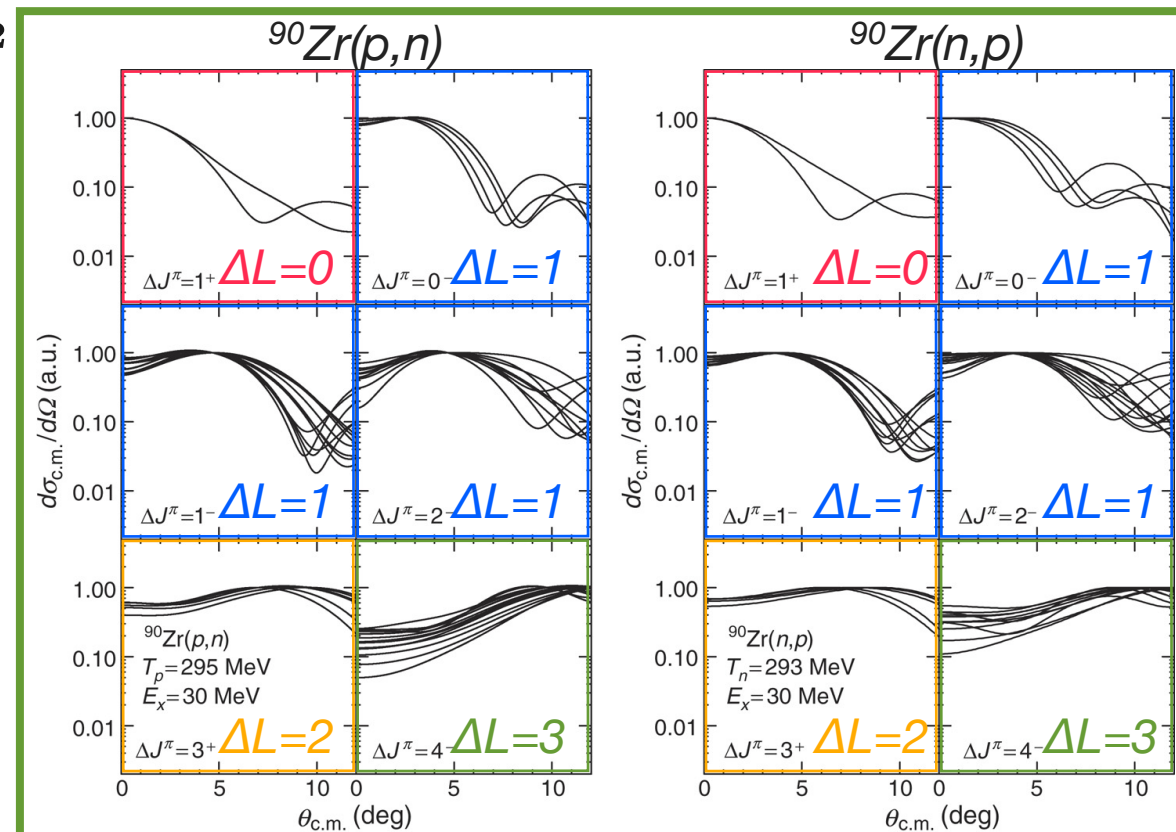
$^{90}\text{Zr}(p,n)$ and $^{90}\text{Zr}(n,p)$
at 300 MeV

Angular distributions, $\sigma_{\Delta J^\pi}^{\text{calc}}$, are prepared for several p-h combinations:

For each $\sigma_{\Delta J^\pi}^{\text{calc}}$, the strength $a_{\Delta J^\pi}$ is determined to minimize the χ^2 -value defined by

$$\chi^2(\omega) = \sum_{\theta} \left[\frac{\sigma^{\text{exp}}(\theta, \omega) - \sum_{\Delta J^\pi} a_{\Delta J^\pi} \sigma_{\Delta J^\pi}^{\text{calc}}(\theta, \omega)}{\delta\sigma^{\text{exp}}(\theta, \omega)} \right]^2$$

- The p-h combination giving the minimum χ^2 is chosen.
- ΔL is limited up to 3 ($\Delta J^\pi=4^-$) due to:
 - $\Delta L_{\text{max}} < \Delta k \cdot R_{\text{Zr}} = 4$
 - limited data points (7 for (p,n))



Results of MDA

For a given ΔL , ΔJ dependence on DWIA cross sections is small:

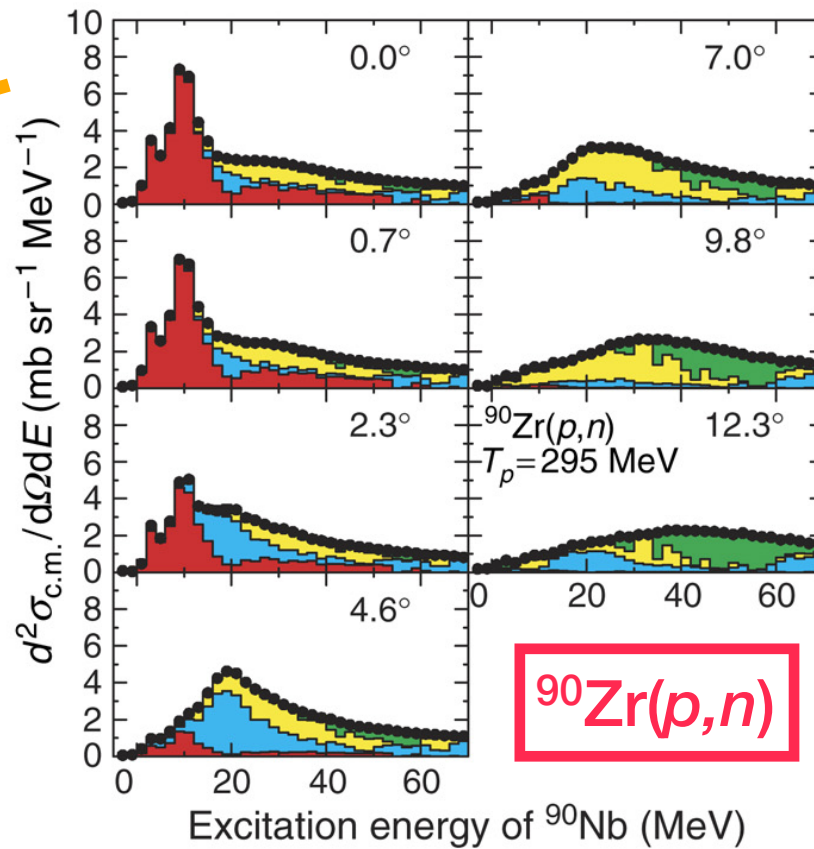
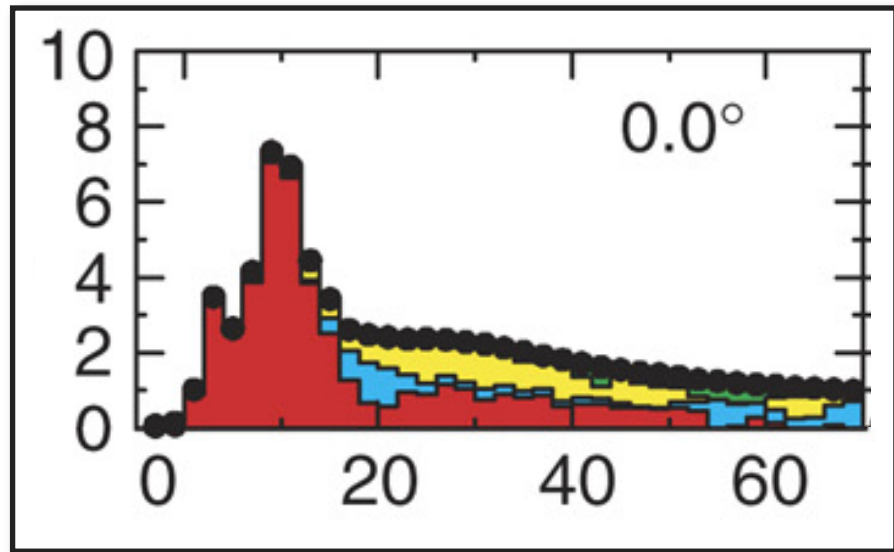
- ΔJ transitions (0^- , 1^- , 2^-) are grouped to the lowest dominant ΔL (1).

ΔJ^π could not be separated in this MDA.

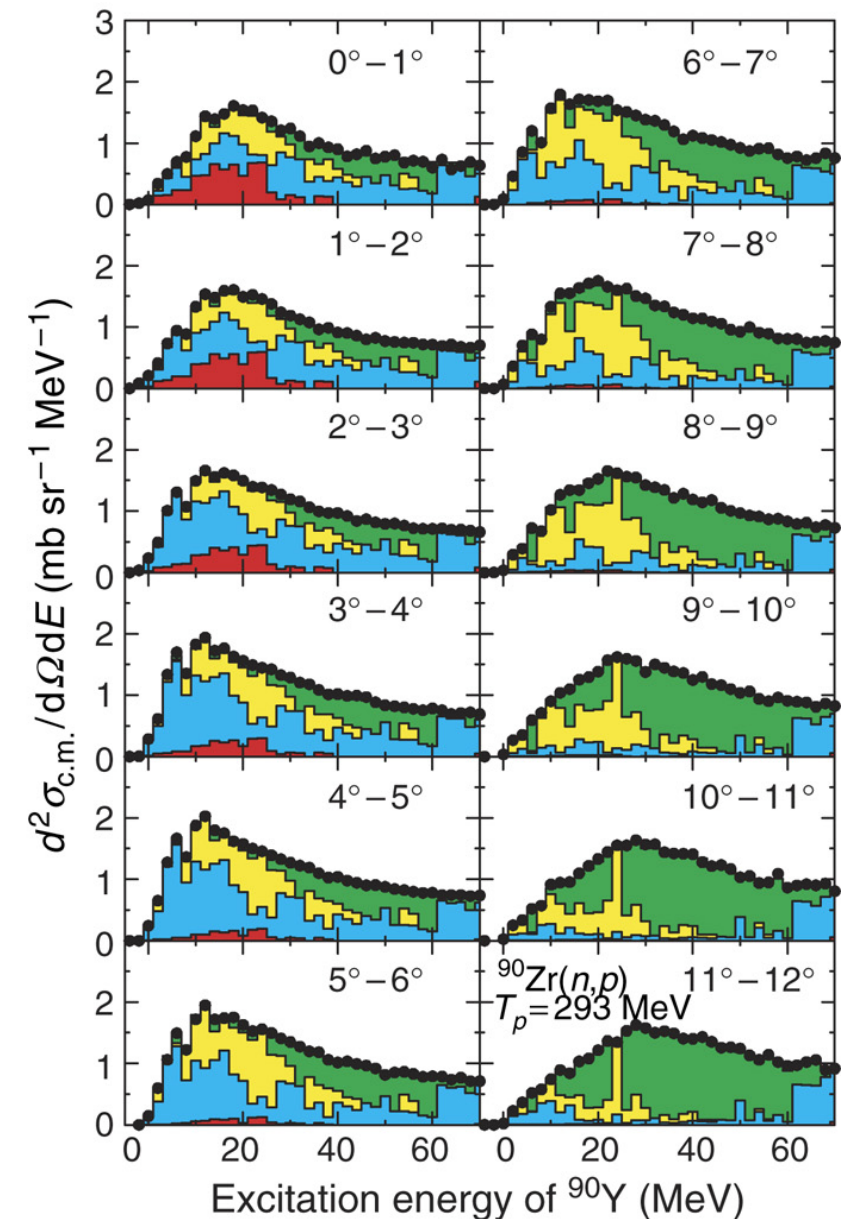
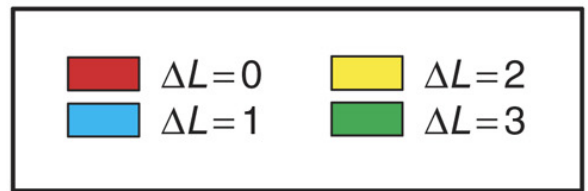
MDA results are in good agreement with the measured cross sections.

- For $^{90}\text{Zr}(p,n)$, a fairly large contribution of $\Delta L=0$ up to $\omega \sim 50$ MeV.
- For $^{90}\text{Zr}(n,p)$, a relatively small $\Delta L=0$ component up to $\omega \sim 30$ MeV.

$^{90}\text{Zr}(n,p)$



$^{90}\text{Zr}(p,n)$

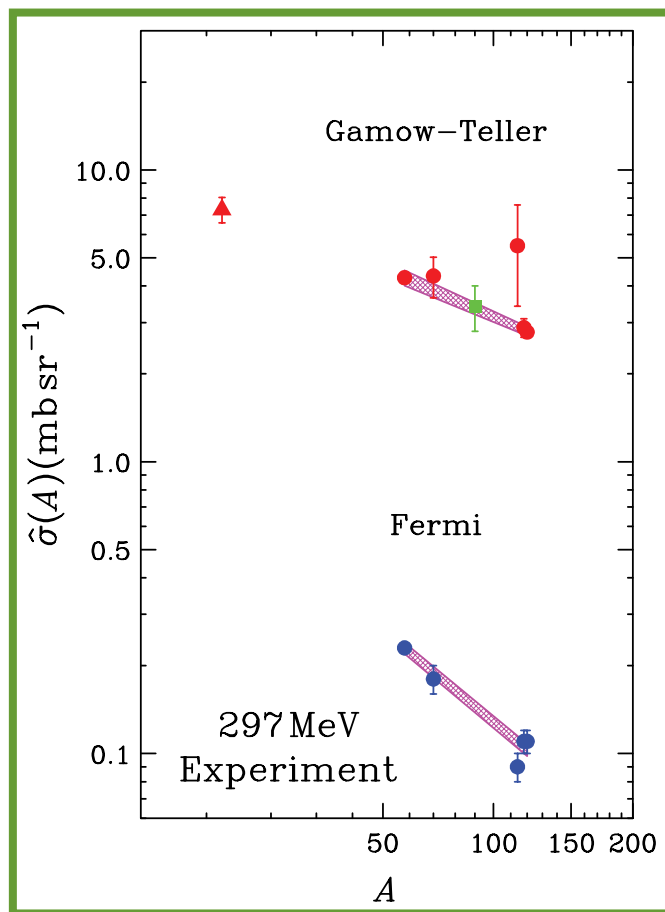


$^{90}\text{Zr}(n,p)$

GT unit cross sections

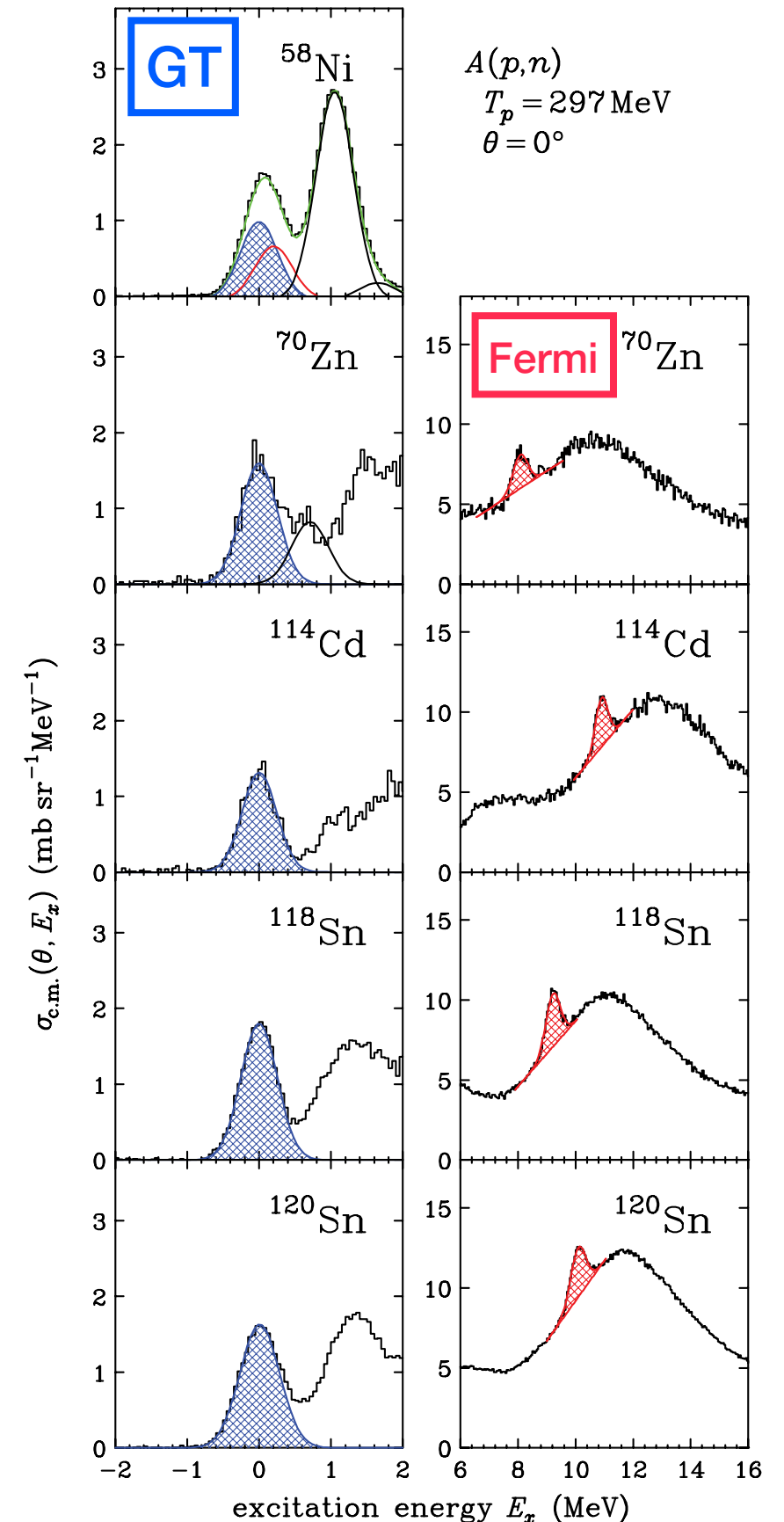
Systematic study for 0° (p,n) cross sections at 297 MeV

- $58 \leq A \leq 120$ ($^{58}\text{Ni} \sim ^{120}\text{Sn}$)
- B(GT)'s are known from beta decay ft values
- GT unit cross sections are obtained as a function of A



$$\hat{\sigma}_{\text{GT}} \text{ for } ^{90}\text{Zr} \rightarrow \hat{\sigma}_{\text{GT}} = 3.36 \pm 0.17 \text{ mb/sr}$$

M. Sasano et al., Phys. Rev. C 79, 024602 (2009).



GT strength distributions

$$\frac{d^2 \sigma_{\Delta L=0}(\theta, \omega)}{d\Omega d\omega} = \hat{\sigma}_{GT} F(\theta, \omega) B(GT; \omega)$$

Experimental B(GT) distributions

(p,n): fairly large B(GT) (0.45 MeV^{-1}) at $\omega=20-60 \text{ MeV}$

(n,p): significant B(GT) at $\omega=20-60 \text{ MeV}$

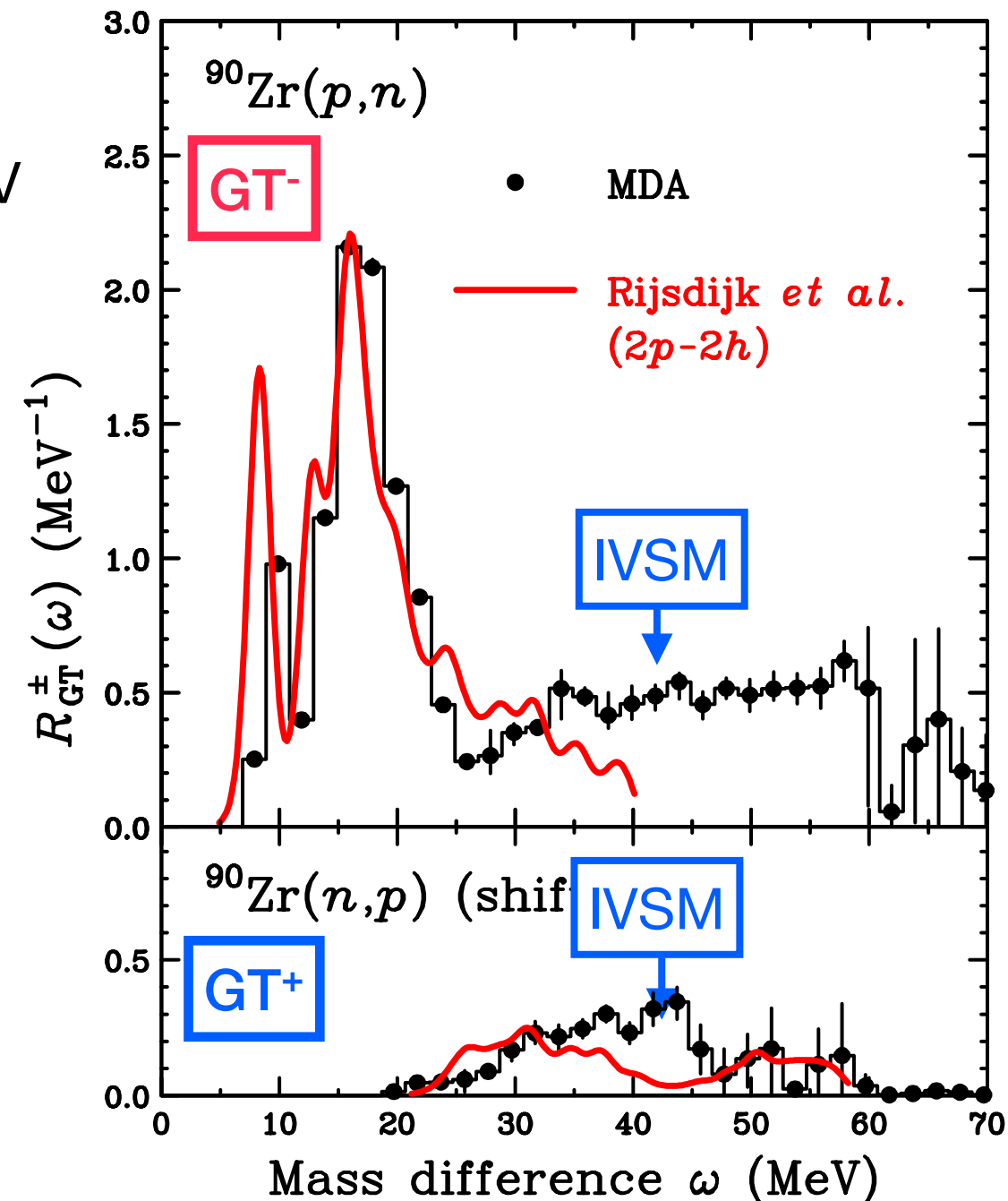
Comparison with calc. including 2p2h effects

Dressed-particle RPA by Rijsdijk et al.

- Predict significant B(GT) for (p,n)
 - supported by the MDA result
- Reproduce both low-lying GT and GTR for (p,n)
- strength at $\sim 30 \text{ MeV}$ for (n,p)

But underestimate at $\omega \sim 40 \text{ MeV}$ for both modes

K.Yako et al., Phys. Lett. B 615, 193 (2005).
M.Ichimura, H.Sakai, T.W., Prog. Part. Nucl. Phys. 56, 446 (2006).



Contribution from IVSM ($2\hbar\omega$) resonances by $r^2\sigma\tau \rightarrow$ should be subtracted.

IVSM contribution

$\Sigma B(\text{GT})$ includes IV spin-monopole (IVSM) strength.

- IVSM : $\Delta J^\pi = 1^+$ transition with $\hat{O}(\text{IVSM}) = r^2 \sigma t_\pm$ (c.f GT: $\hat{O}(\text{GT}) = \sigma t_\pm$)
- $\Delta L = 0$: indistinguishable from GT in a MDA

Estimation of IVSM

IVSM contribution is estimated in DWIA.

- The transition matrix was calculated by using the operator:

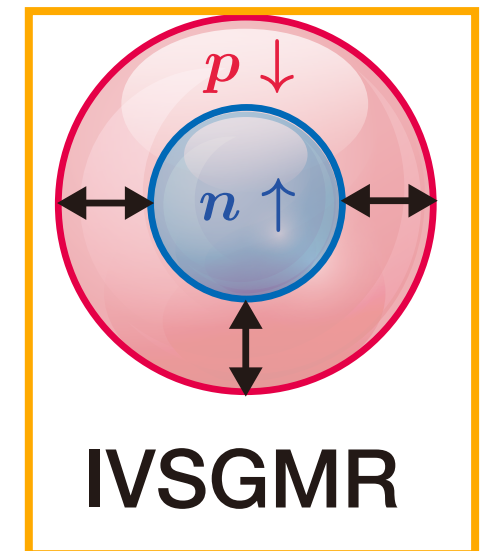
$$\hat{O}(\text{IVSM}) = r^2 \sigma t_\pm$$

- In terms of p-h excitations from $|0\rangle$ to $|JM\rangle$, the normal-mode wave function is:

$$\begin{aligned} |JM\rangle &= \sum_{ph} \chi_{JM}^{ph} |ph; JM\rangle \\ &= \sum_{ph} \chi_{JM}^{ph} [a_p^\dagger a_h]_{JM} |0\rangle \end{aligned}$$

where

$$\chi_{JM}^{ph} = \frac{\langle ph; JM | \hat{O}_{LJ}^\dagger | 0 \rangle}{\sqrt{\sum_{ph} |\langle ph; JM | \hat{O}_{LJ}^\dagger | 0 \rangle|^2}}$$



For IVSM:

$$\hat{O}_{LJ} = \hat{O}(\text{IVSM})$$

$$L = 0, J = 1$$

This method exhausts the (non-energy-weighted) sum rule (maximum IVSM contribution).

IVSM contribution

The calculated IVSM cross section in DWIA is

(p,n) t₋ mode : 4.2 ± 0.9 in the GT unit

(n,p) t₊ mode : 2.5 ± 0.3 in the GT unit

- The sum-rule value has been assumed (maximum contribution of IVSM).

By subtracting the IVSM contribution, quenching factor becomes:

$$Q \equiv \frac{S_{\text{GT}}^- - S_{\text{GT}}^+}{3(N - Z)} = 0.86 \pm 0.07$$

→ 86±7 % of the sum rule value of 3(N-Z)=30 has been found up to ω=56 MeV

- Configuration mixing : dominant
- Δ-hole : minor (~ 10%) effect (but might be not negligible)

Landau-Migdal parameters, g'_{NN} and $g'_{N\Delta}$

M. Ichimura, H. Sakai, T.W., Prog. Part. Nucl. Phys. 56, 446 (2006).

Landau-Migdal interaction at $q=0$

$$V_{\text{LM}} = \frac{f_{\pi NN}^2}{m_\pi^2} \underline{g'_{NN}} + \frac{f_{\pi NN} f_{\pi N\Delta}}{m_\pi^2} \underline{g'_{N\Delta}}$$

repulsion between particle and hole (ph)

coupling between ph and Δh

LM parameter g'_{NN}

Determine the p-h repulsion

Sensitive to GTR peak position

- $g'_{NN} = 0.6 \pm 0.1$

LM parameter $g'_{N\Delta}$

Determine the coupling to Δ

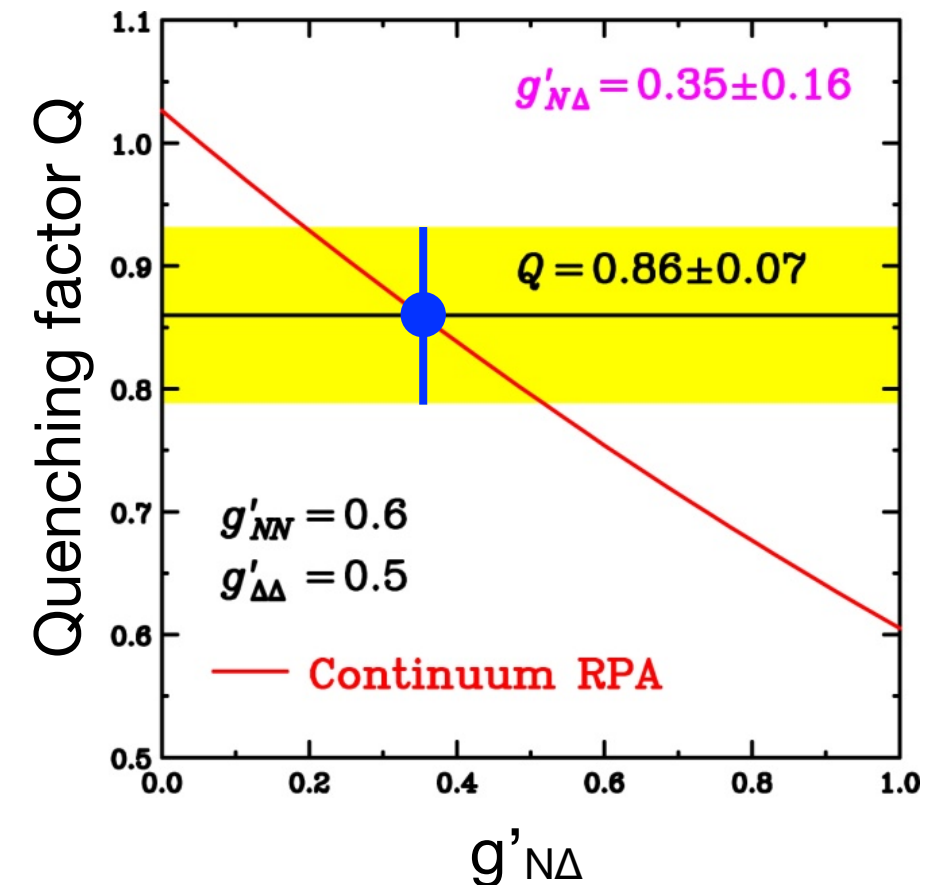
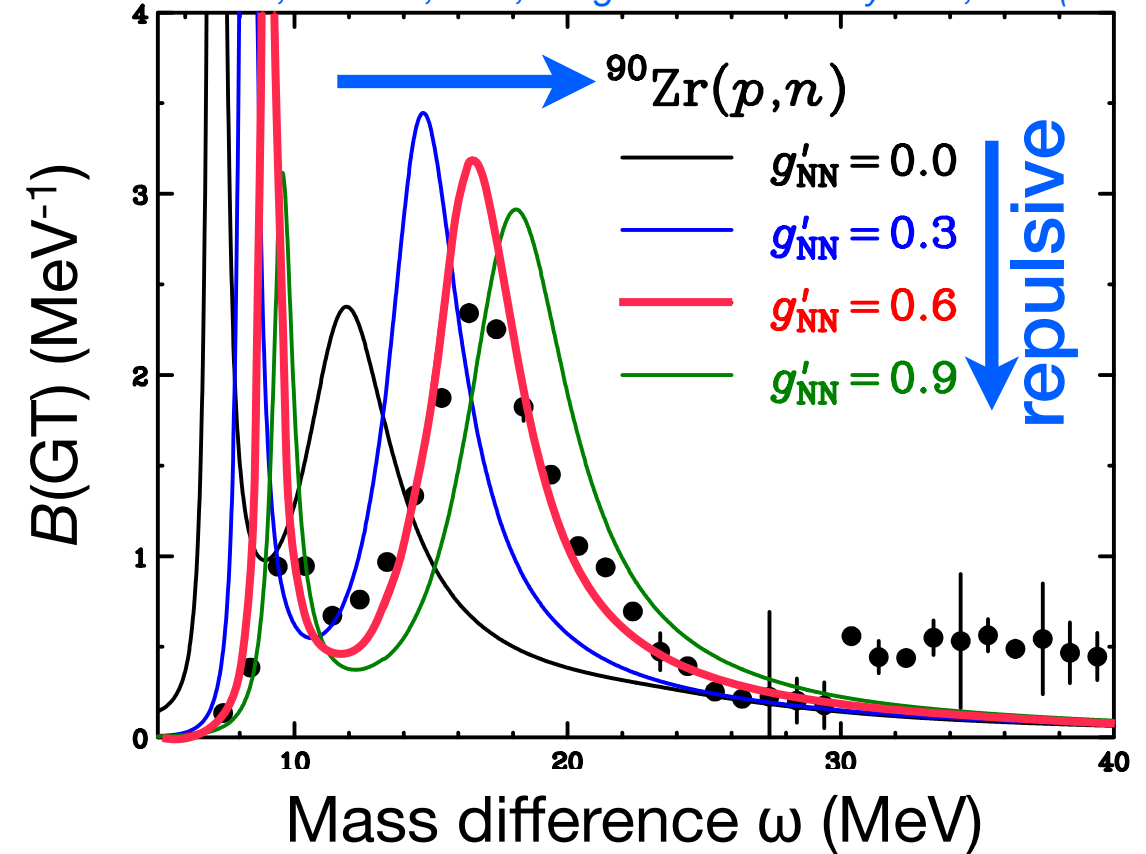
Sensitive to the GT quenching factor Q

- $g'_{N\Delta} = 0.35 \pm 0.16$

$g'_{NN} > g'_{N\Delta}$

❖ The universality, $g'_{NN}=g'_{N\Delta}$, does not hold.

❖ Configuration mixing effect is dominant.



Spin-isospin excitations/GRs with higher multipoles

Higher multipole modes and sum rule

C. Gaarde, Nucl. Phys. A 396, 127c (1983).

Up to now, we have focused on $\Delta L=0$ GT mode

In (p,n) spectra, finite multipole ($L \geq 1$) modes are also observed

With increasing θ (q), ΔL is also increased.

- Dipole mode with $\Delta L=1$ and $\Delta S=0$
- Spin-dipole (SD) mode with $\Delta L=1$ and $\Delta S=1$
($\Delta J^\pi = 0^-, 1^-, 2^-$)

Isovector spin-dipole (SD)

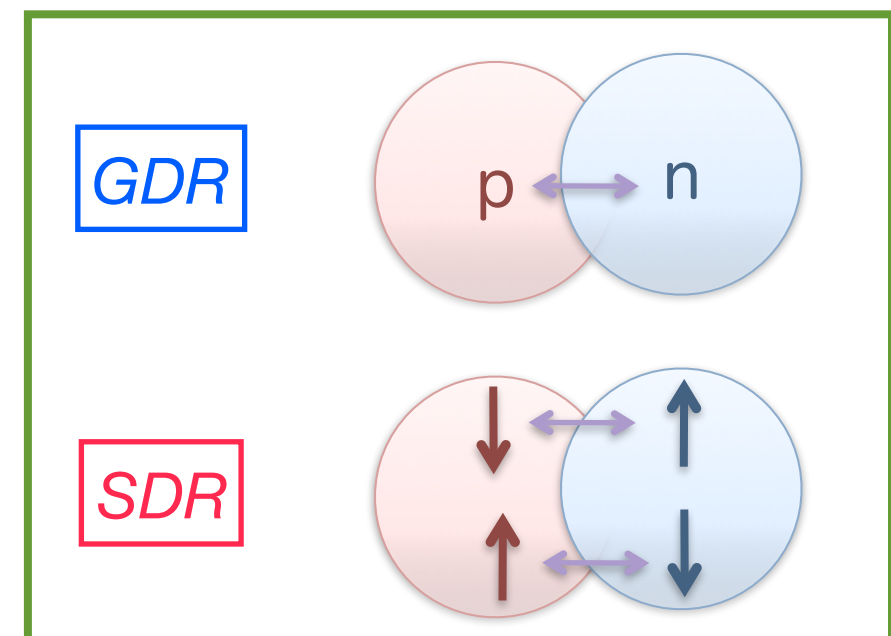
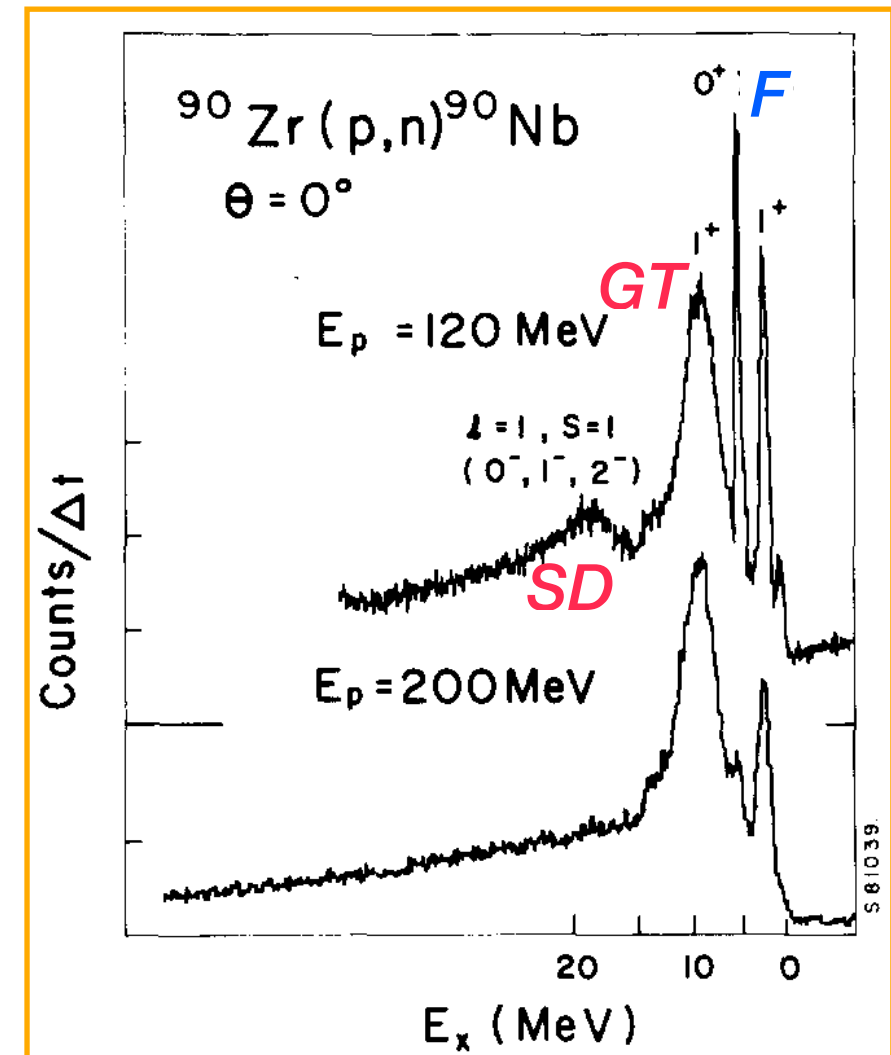
$\Delta S=1$ and $\Delta T=1$

In macroscopic picture

- Dipole oscillation of $p \uparrow$ ($p \downarrow$) against $n \downarrow$ ($n \uparrow$)

For SD, what can we learn from:

- *sum rule (total strength including SDR)*
- *strength distributions*



Higher multipole modes and sum rule

Higher-multipole spin-isospin transition operators:

- IV Spin-**scalar** $\hat{O}_{\pm} = \sum_{\mathbf{k}} r_{\mathbf{k}}^{\ell} Y_{\ell}(\hat{r}_{\mathbf{k}}) t_{\pm}(\mathbf{k})$
- IV Spin-**vector** $\hat{O}_{\pm} = \sum_{\mathbf{k}} r_{\mathbf{k}}^{\ell} [Y_{\ell}(\hat{r}_{\mathbf{k}}) \otimes \sigma(\mathbf{k})]_{J\pi} t_{\pm}(\mathbf{k})$

Model-independent sum-rule

$$\underbrace{\sum_m \left| \langle m | \hat{O}_{-} | 0 \rangle \right|^2}_{\equiv S^{-}} - \underbrace{\sum_n \left| \langle n | \hat{O}_{+} | 0 \rangle \right|^2}_{\equiv S^{+}} = \frac{(2J+1)}{4\pi} \left[\underset{\text{neutron}}{N \langle r^{2\ell} \rangle_n} - \underset{\text{proton}}{Z \langle r^{2\ell} \rangle_p} \right] \times \begin{cases} 1 & : \text{scalar} \\ 3 & : \text{vector} \end{cases}$$

(p, n) ↓ (n, p) ↓

SD sum-rule ($\Delta L = \Delta S = \Delta T = 1$, summed over $J=0^{-}$, 1^{-} , and 2^{-})

$$S_{-} - S_{+} = \frac{9}{4\pi} (N \langle r^2 \rangle_n - Z \langle r^2 \rangle_p)$$

from charge radius

Sum-rule value gives

- rms radius of neutron distribution: $\sqrt{\langle r^2 \rangle_n}$
- neutron skin thickness: $\delta_{np} = \sqrt{\langle r^2 \rangle_n} - \sqrt{\langle r^2 \rangle_p}$

SD strengths for ^{90}Zr

In MDA for $^{90}\text{Zr}(p,n)$ and $^{90}\text{Zr}(n,p)$, the $\Delta L=1$ strengths are dominant at $\theta \sim 4^\circ$

- Resonance-like structure \rightarrow *SD resonance (SDR) is clearly observed in (p,n)*

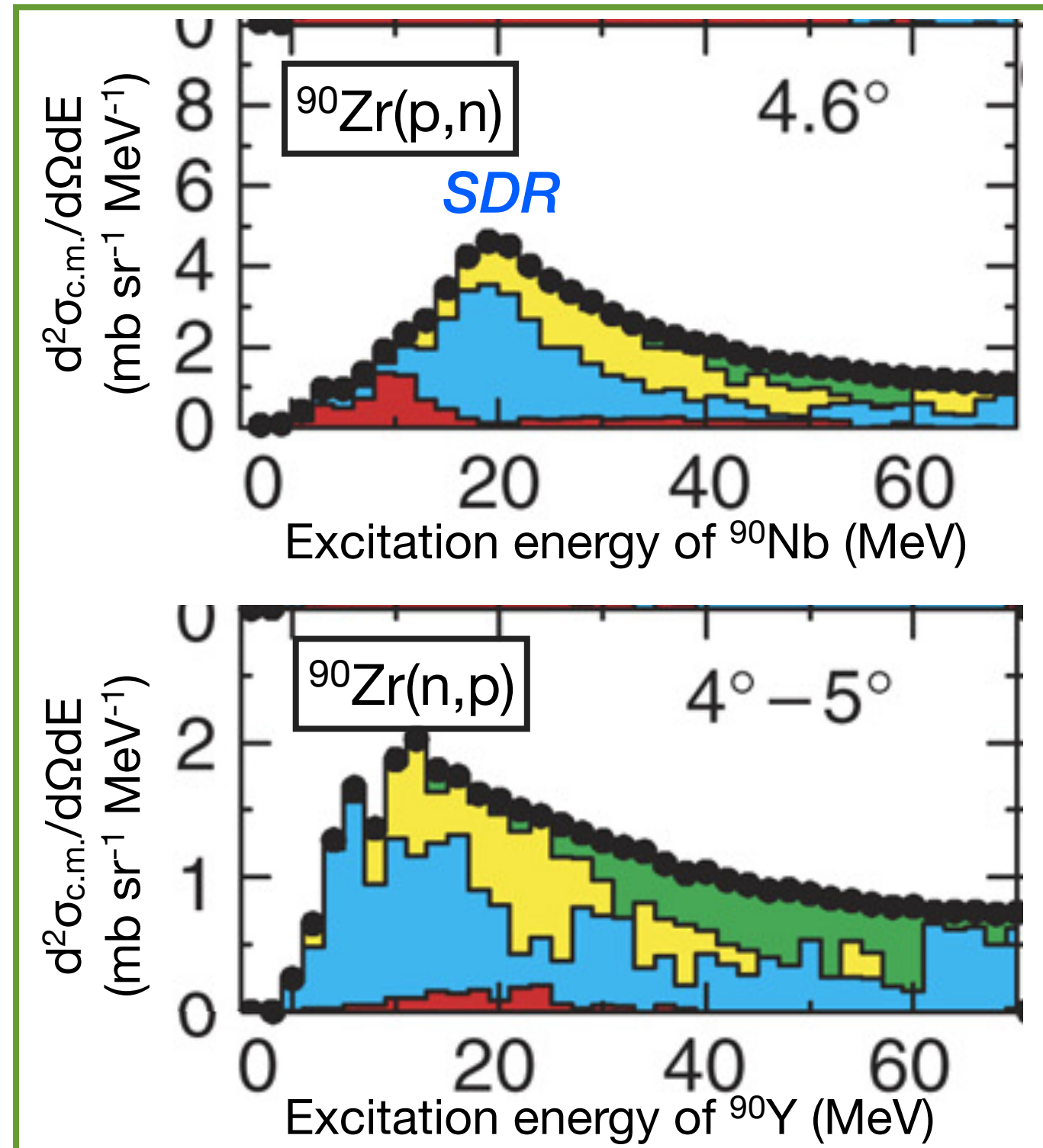
Proportionality relation (assumption)

- Maximum c.s at $\theta \sim 4^\circ$
- Proportionality relation

$$\sigma_{\text{SD},\pm}(\simeq 4^\circ) = \hat{\sigma}_{\text{SD}\pm} B(\text{SD}\pm)$$

- SD unit c.s. are calculated in DWIA
 - (p,n) : $\hat{\sigma}_{\text{SD}_-} = 0.27 \text{ mb/sr/fm}^2$
 - (n,p) : $\hat{\sigma}_{\text{SD}_+} = 0.26 \text{ mb/sr/fm}^2$

SD strengths, $B(\text{SD}\pm)$, have been deduced from $\sigma_{\text{SD}} (\Delta L=1)$



SD sum-rule and neutron skin thickness

K. Yako et al., PRC 74, 051303(R) (2006).

Running sum of SD strength

$$S_{\pm} = \int_0^{E_x} \frac{dB(\text{SD}_{\pm})}{dE} dE$$

Exp. values approach

HF+RPA values at 50 MeV

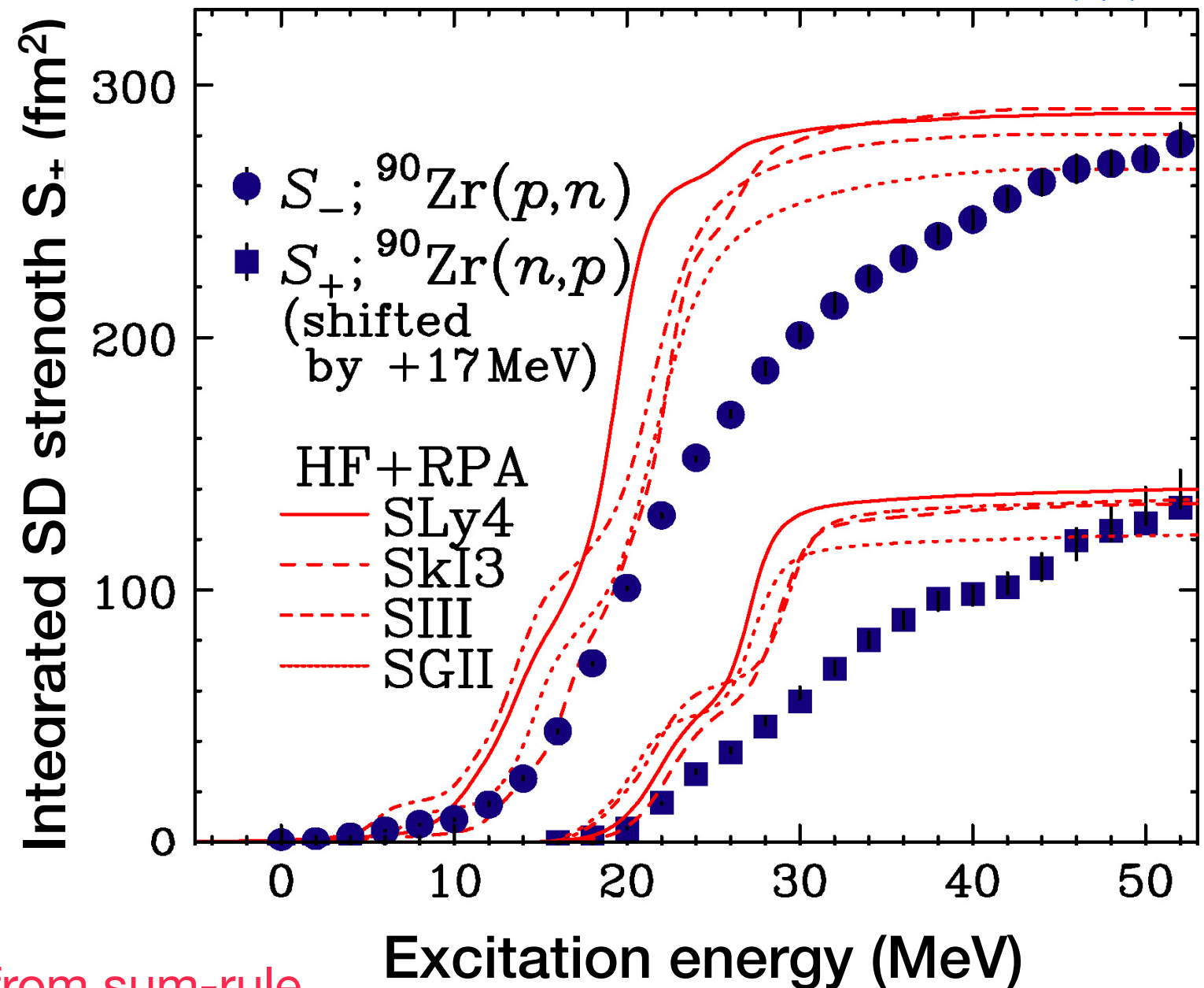
Sum-rule value

$$\blacklozenge S_- - S_+ = 148 \pm 13 \text{ fm}^2$$

Rms radius

$$\sqrt{\langle r^2 \rangle_p} = 4.19 \text{ fm}$$

$$\sqrt{\langle r^2 \rangle_n} = 4.26 \pm 0.04 \text{ fm from sum-rule}$$



- Neutron skin thickness : $\delta_{np} = \sqrt{\langle r^2 \rangle_n} - \sqrt{\langle r^2 \rangle_p} = 0.07 \pm 0.04 \text{ fm}$
- cf. goal of parity violation electron scattering: ± 0.04 (1%)
- How about SD strength distributions?

SD strength distributions

Exp. strength

Extends up to 50 MeV

- Configuration mix.

Single bump

HF+RPA (1p1h)

Underestimation at $E_x > 25$ MeV

- 2p2h is important

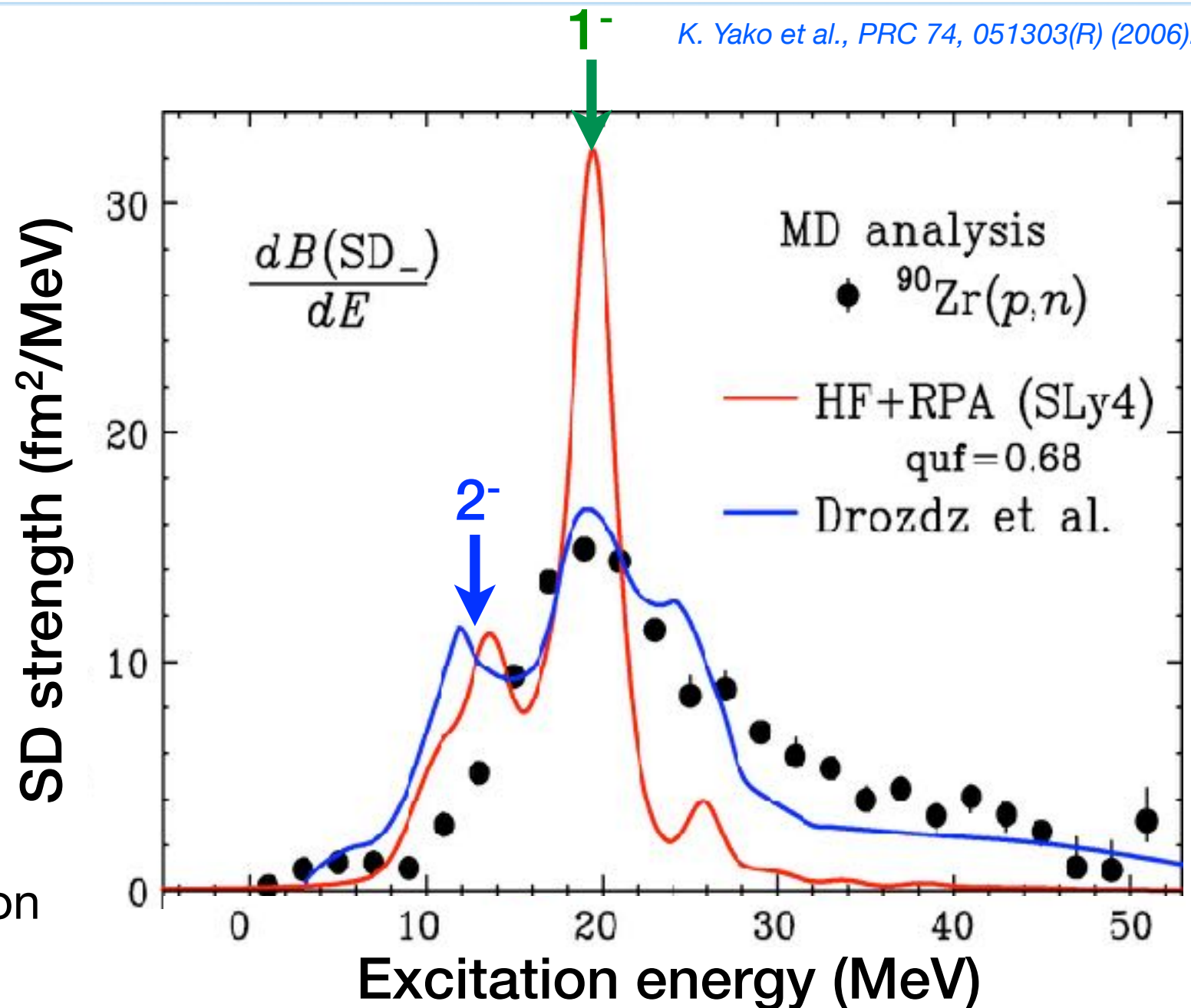
Three bumps

- $E_x(2^-) > E_x(1^-)$

Second-order RPA

Reasonably reproduce in whole region

Three bumps



Each ΔJ^π (0^- , 1^- , 2^-) distributions \rightarrow Inconsistent (tensor correlation?)

Exercise: The calculation predicts a definite sequence, i.e. 2^- , 1^- , 0^- , with increasing excitation energies. This reflects the same systematics of the unperturbed p-h states. Show this systematics referring Appendix C of this lecture.

Extension of Landau-Migdal interaction

A.B.Migdal, "Theory of Finite Systems and Application to Atomic Nuclei" (1967).

A simple extension of Landau-Migdal interaction is to introduce Tensor interaction as:

$$V_{\text{LM}}^{\sigma\tau} = C_0(\tau_1 \cdot \tau_2) [g'(\sigma_1 \cdot \sigma_2) + \underbrace{h' S_{12}(\hat{q})}_{\text{tensor term}}]$$

Since the tensor operator $S_{12}(\hat{q})$ can be expressed as

Exercise: Show this equation.

$$S_{12}(\hat{q}) \equiv 3(\sigma_1 \cdot \hat{q})(\sigma_2 \cdot \hat{q}) - \sigma_1 \cdot \sigma_2$$



$$= 2(\sigma_1 \cdot \hat{q})(\sigma_2 \cdot \hat{q}) - (\sigma_1 \times \hat{q}) \cdot (\sigma_2 \times \hat{q})$$

$$\sigma_1 \cdot \sigma_2 = (\sigma_1 \cdot \hat{q})(\sigma_2 \cdot \hat{q}) + (\sigma_1 \times \hat{q}) \cdot (\sigma_2 \times \hat{q})$$

the Landau-Migdal interaction becomes:

$$V_{\text{LM}}^{\sigma\tau} = C_0(\tau_1 \cdot \tau_2) [(g' + 2h')(\sigma_1 \cdot \hat{q})(\sigma_2 \cdot \hat{q}) + (g' - h')(\sigma_1 \times \hat{q}) \cdot (\sigma_2 \times \hat{q})]$$

0^- and 2^- (spin-longitudinal) 1^- and 2^- (spin-transverse)

- spin-longitudinal : **strengthen** the residual interaction → **peak shift to high- ω (hardening)**
- spin-transverse : **weaken** the residual interaction → **peak shift to low- ω (softening)**

Spin-dipole resonance (SDR)

- 0^- (weak) : pure spin-longitudinal
- 1^- : pure spin-transverse
- 2^- : mixed

Tensor force can induce mode-dependent effects

- 2^- : almost cancelled
 - 1^- : peak shift to lower ω
- } → $E_x(2^-) \sim E_x(1^-)$?

Separation of SDR into each J^π

Separation of SDR ($L=1$) into 0^- , 1^- , 2^- is important

- Tensor effects depends on J^π

Normal multipole decomposition

- Separate into each L component
 - Works very well to extract GT ($L=0$)
- Could NOT separate into J^π with same L
 - Angular distributions are governed by L

Idea to separate SDR into each J^π

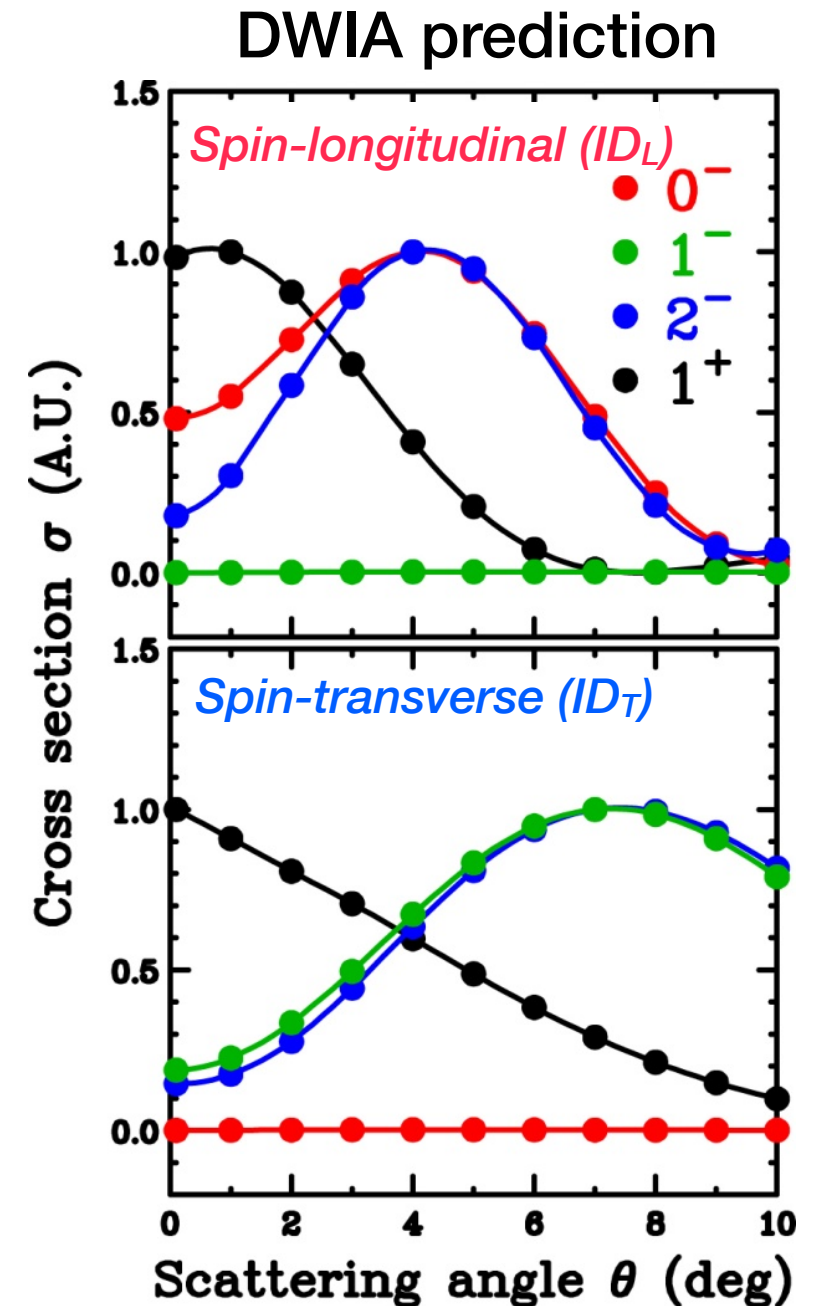
- Polarization observables are sensitive to J^π
- Separate c.s. (I) into longitudinal (ID_L) - transverse (ID_T)

$$ID_L(0^\circ) = \frac{I}{4}(1 - 2D_{NN} + D_{LL})$$

$$ID_T(0^\circ) = \frac{I}{2}(1 - D_{LL})$$

- 0^- : Spin-longitudinal (ID_L) only
- 1^- : Spin-transverse (ID_T) only
- 2^- : Both

Multipole decomposition for longitudinal (ID_L) and transverse (ID_T) c.s.
 → Can separate/specify not only L , but also J^π



Results of multipole (L and J^π) decomposition for ^{208}Pb

T.W. et al., Phys. Rev. C 85, 064606 (2012).

non-spin-flip
 $\Delta S = 0$

spin-flip
 $\Delta S = 1$

$$I = ID_0 + ID_L + ID_T$$

Note:

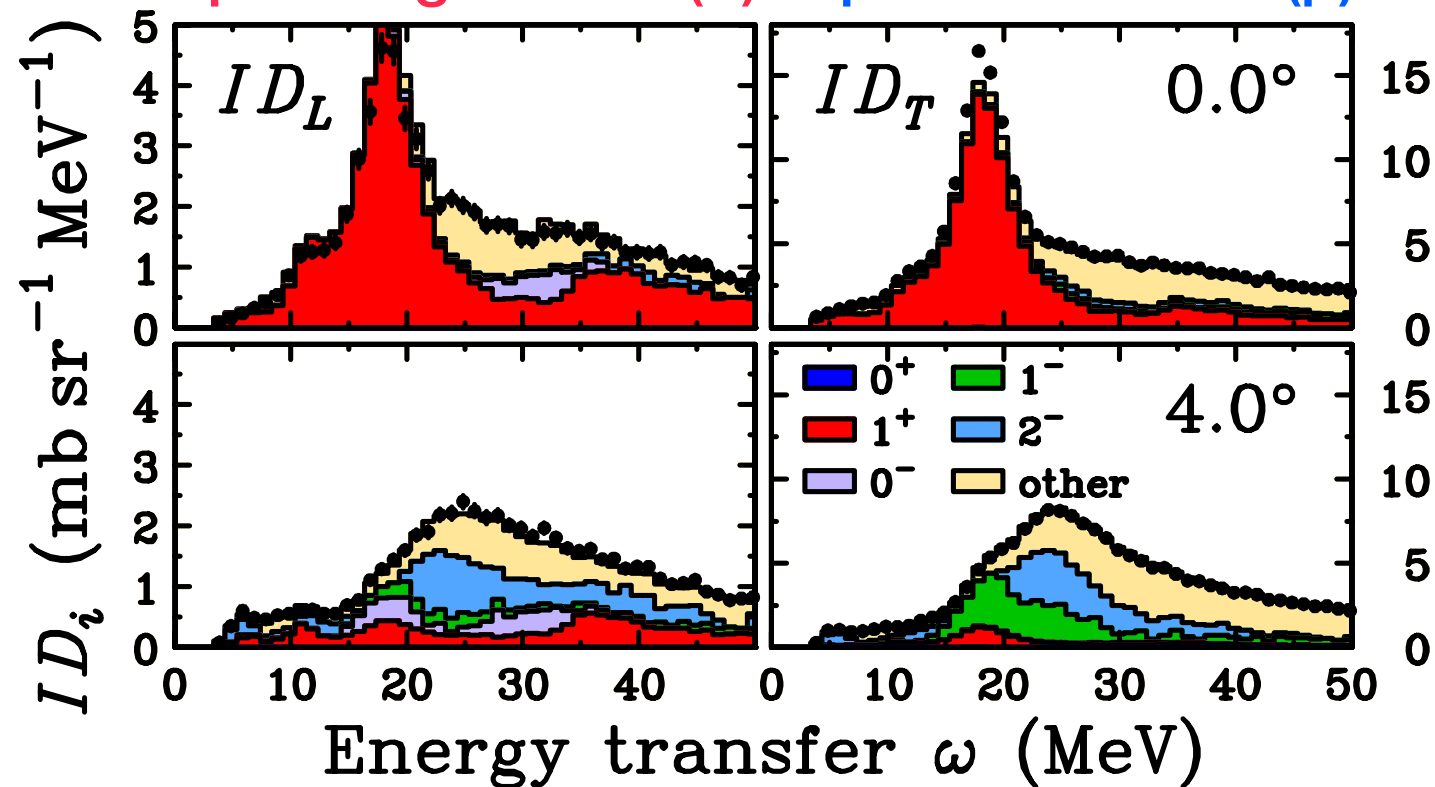
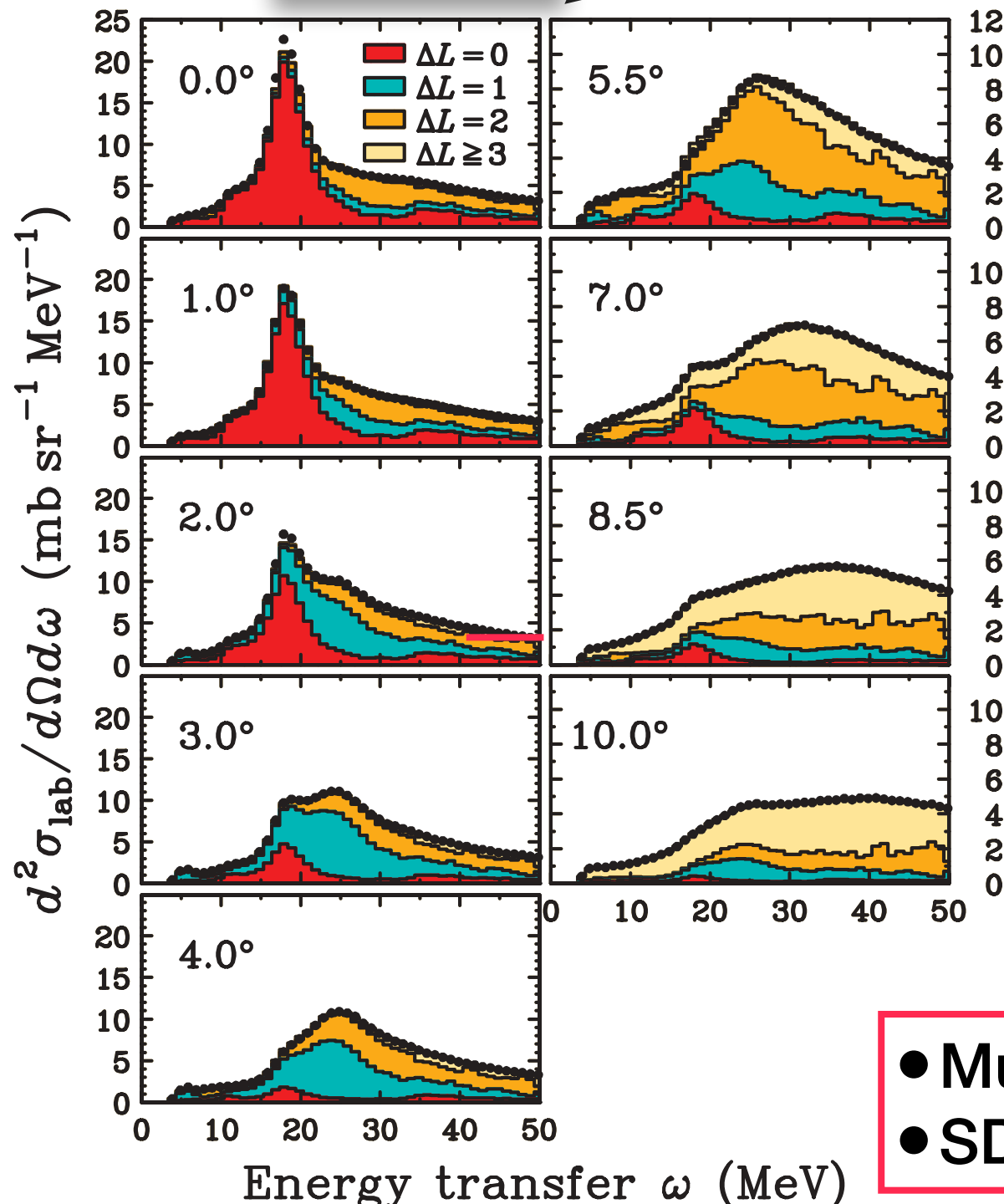
$$ID_L \equiv ID_q$$

$$ID_T \equiv ID_p + ID_n$$

$I(\theta) \rightarrow \Delta L$

Spin-longitudinal (π)

Spin-transverse (ρ)



$\Delta L=0: 1^+$

$\Delta L=0: 1^+$

$\Delta L=1: 0^-$ and 2^-

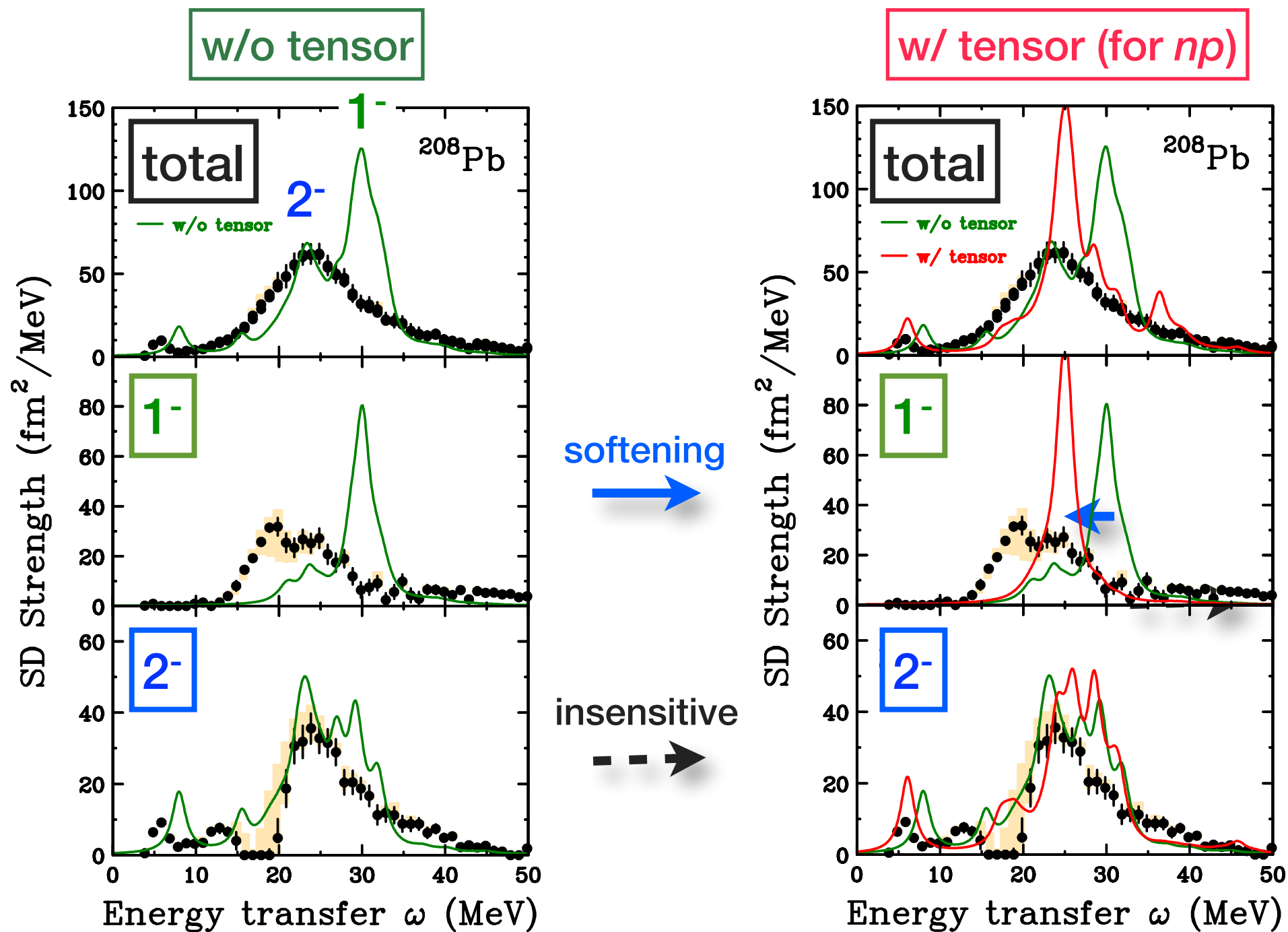
$\Delta L=1: 1^-$ and 2^-

ID_L and $ID_T \rightarrow \Delta J^\pi$

- Multipole (J^π) decomposition is successful
- SD strength is *separated* into 0^- , 1^- , and 2^-

Tensor force effects on SDR

Tensor force : $V^T \rightarrow J^\pi$ dependent effects on SDR in the calculations



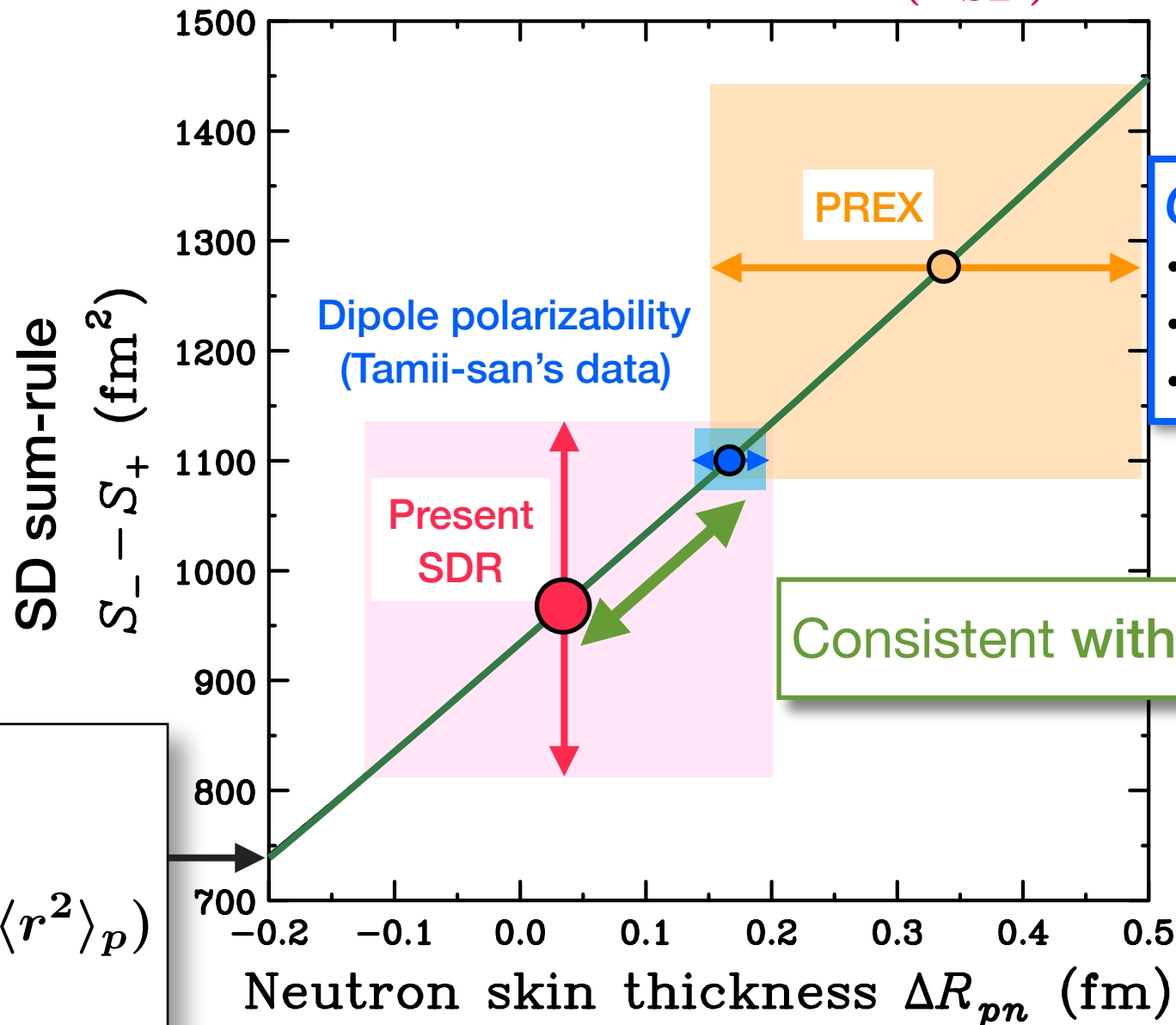
Note:
We focus on 1^- and 2^- strengths for simplicity. (since 0^- strength is relatively weak.)

- Softening on 1^- is reproduced by considering the tensor correlation.
 - V^T (tensor for np) $\sim 200 \text{ MeV fm}^5$

Spin-dipole sum rule for ^{208}Pb

Experimental S_- value : $S_- = 1004 \pm 22(\text{stat.}) \pm 163(\hat{\sigma}_{\text{SD}}) \text{ fm}^2$

- Quenching by Δ is expected to be $\sim 8\%$ \rightarrow Corrected $S_- = 1085 \text{ fm}^2$
- S_+ is expected to be 11% of S_- $\rightarrow S_+ = 116 \text{ fm}^2$
- Estimated value: $S_- - S_+ = 969 \pm 24(\text{stat.}) \pm 163(\hat{\sigma}_{\text{SD}}) \text{ fm}^2$
 $\pm 165 \text{ cm}^2$ ($\delta(\hat{\sigma}_{\text{SD}})$ is dominant)



Open questions/problems

- Δ effects on SD strength
- SD strength for (n,p)
- Precise determination of $\hat{\sigma}_{\text{SD}}$

SD sum rule

$$S_- - S_+ = \frac{9}{4\pi} (N \langle r^2 \rangle_n - Z \langle r^2 \rangle_p)$$

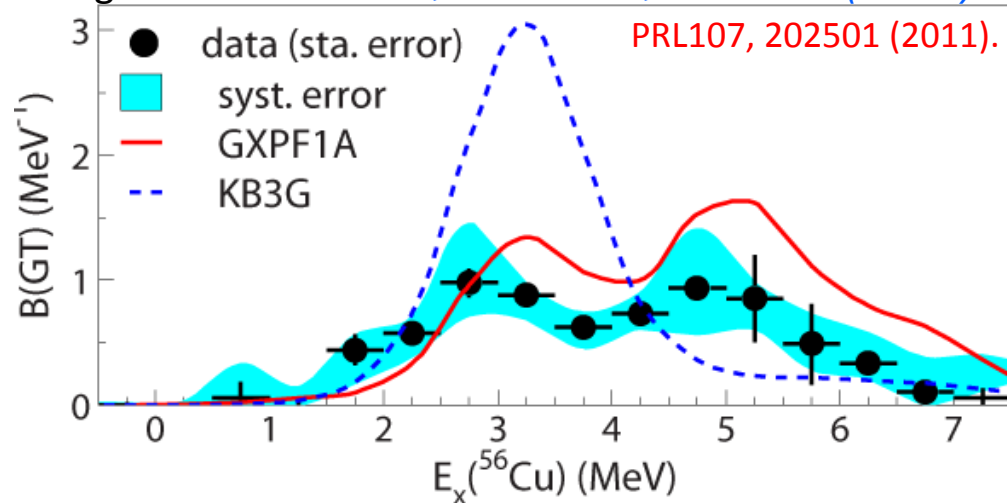
Final Remark

Spin-isospin responses for unstable nuclei

- *Isospin dependence*
 - *Skin/halo effect (Fermi-level diff.)*
- on resonance/residual int. will be known soon.

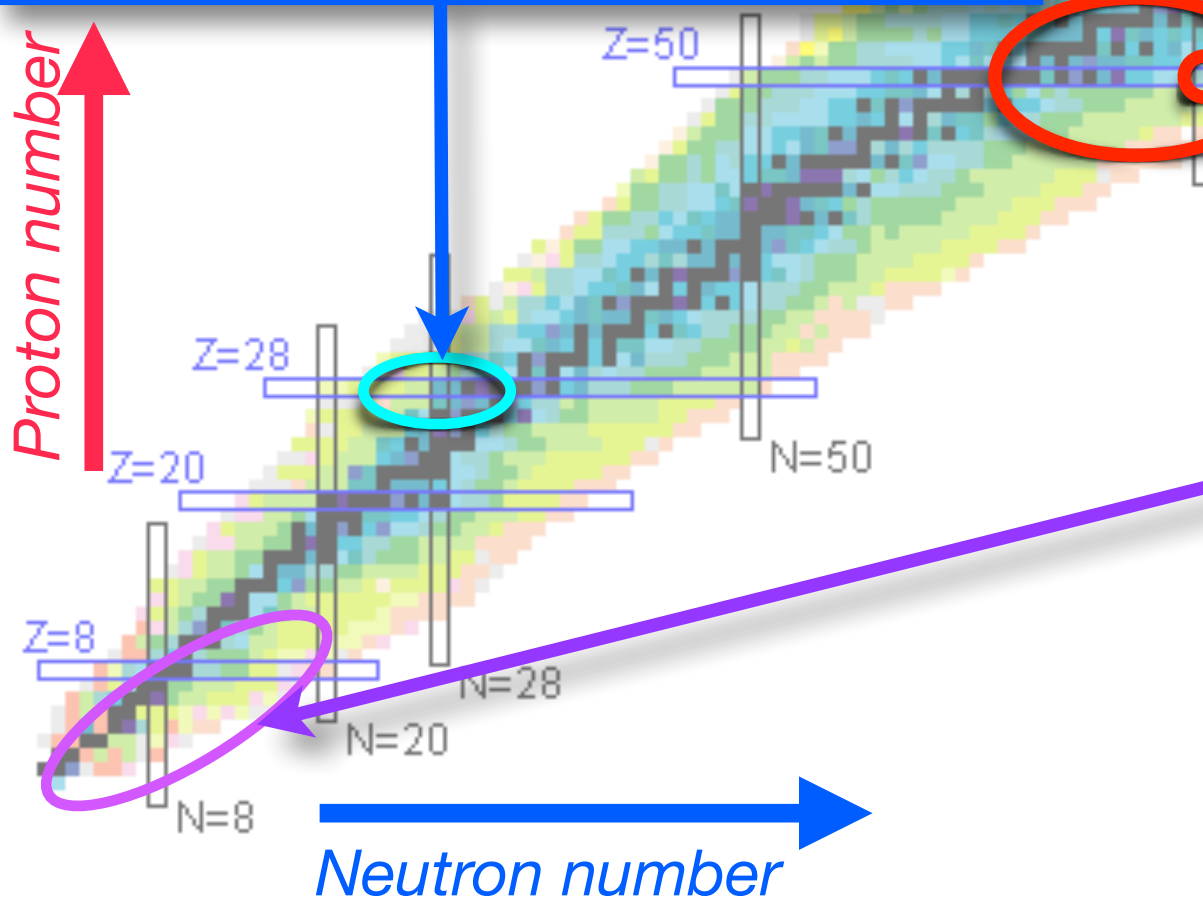
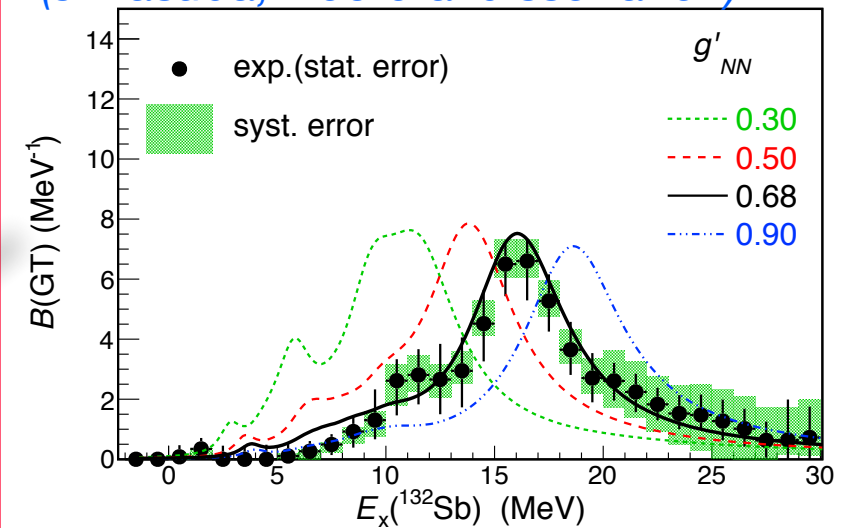
$^{56}\text{Ni}(p,n)$; GT

M. Sasano et al., PRL 107, 202501 (2011).



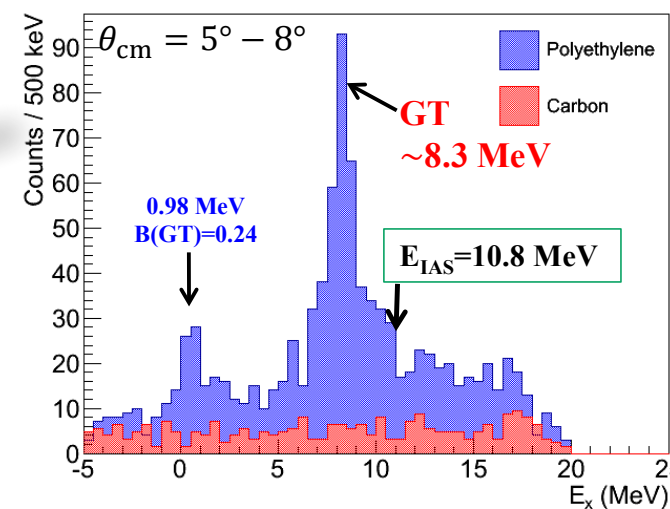
$^{132}\text{Sn}(p,n)$; GT

J. Yasuda, M. Sasano et al.,
(J. Yasuda, Doctoral dissertation)



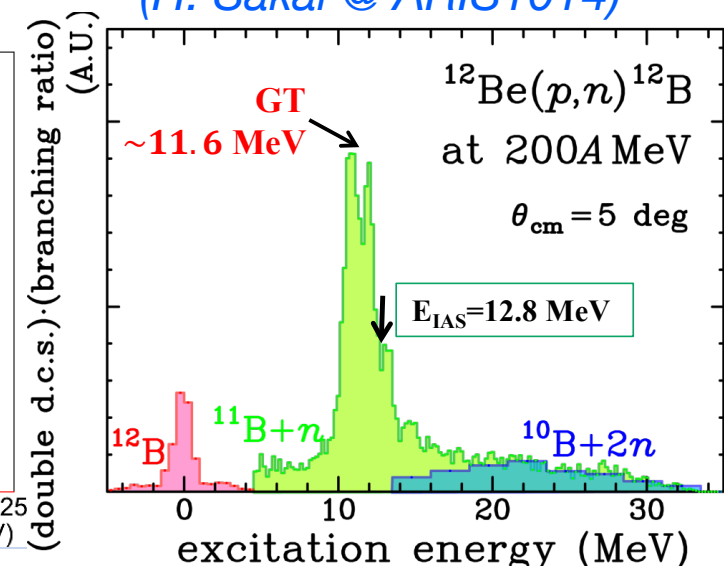
$^8\text{He}(p,n)$; GT

M. Kobayashi et al.,
(H. Sakai @ ARIS1014)



$^{12}\text{Be}(p,n)$; GT

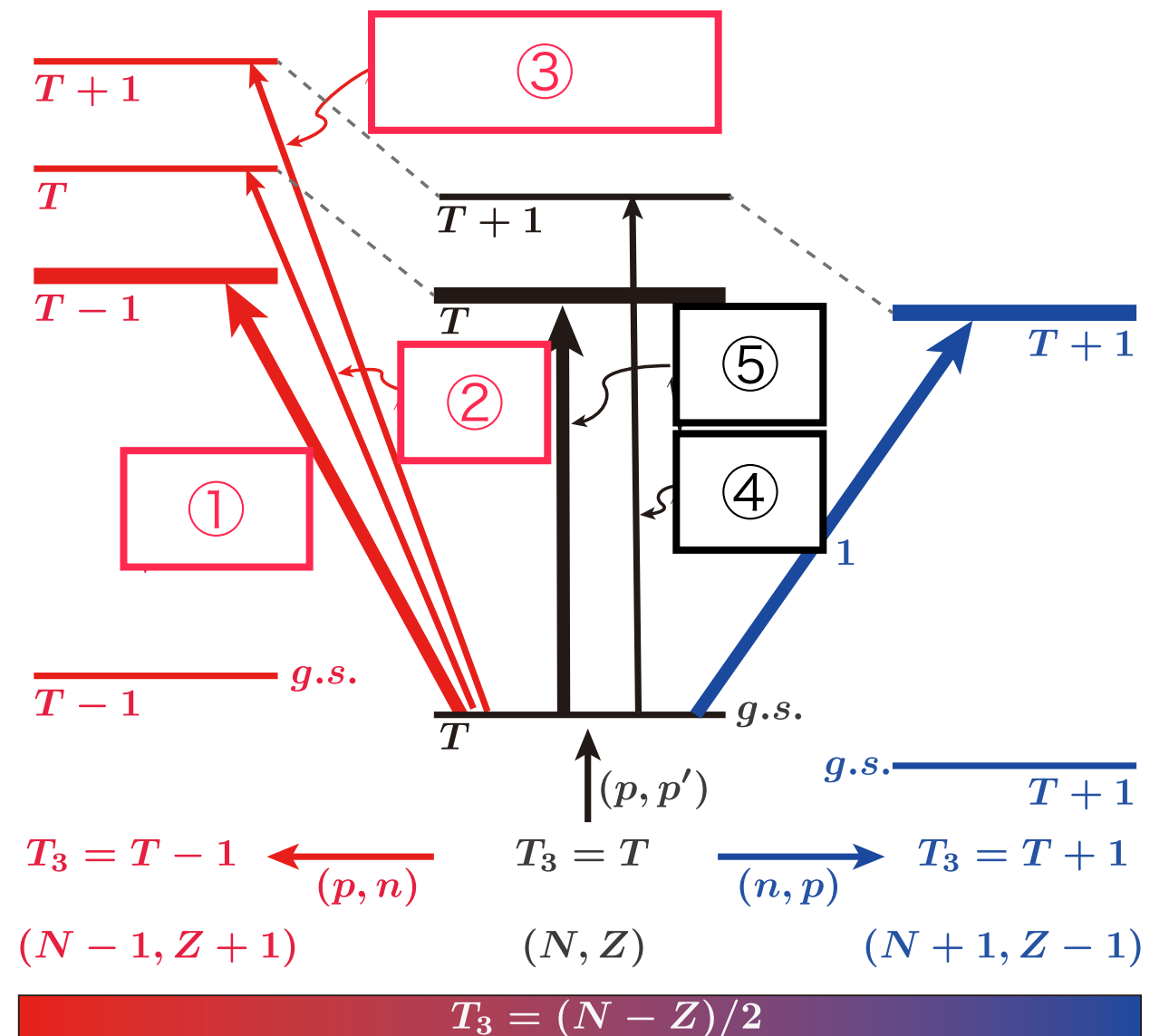
K. Yako et al.,
(H. Sakai @ ARIS1014)



Homework #3

Homework #3

1. Let us consider the isospin transitions in a nucleus with ground-state isospin $T=T_3=(N-Z)/2$. Each transitions matrix element is proportional to the relevant isospin Clebsh-Gordan coefficient $(T T 1 -1 | 1 -1)$. Calculate this isospin coefficients for the transitions ①–⑤ and show that, in the (p,n) reaction on a $N>Z$ nuclei, the $T-1$ state is predominantly excited compared with the T and $T+1$ states.



Homework #3 (cont'd)

2. Show the following equality.

$$\sigma_1 \cdot \sigma_2 = (\sigma_1 \cdot \hat{q})(\sigma_2 \cdot \hat{q}) + (\sigma_1 \times \hat{q}) \cdot (\sigma_2 \times \hat{q})$$

3. The kinetic energy resolution, ΔT_n , by the TOF method is related to the uncertainties of both of timing, t , and flight path length, L , as

$$\frac{\Delta T_n}{T_n} = \gamma(\gamma + 1) \sqrt{\left(\frac{\Delta t}{t}\right)^2 + \left(\frac{\Delta L}{L}\right)^2}$$

where Δt and ΔL are uncertainties of t and L , respectively, and γ is the Lorentz factor. Show this relation.

4. For the SD strength distributions, the calculation predicts a definite sequence, i.e. 2^- , 1^- , 0^- , with increasing excitation energies. This reflects the same systematics of the unperturbed p-h states. Show this systematics referring Appendix C of this lecture.

Appendix A

General features of 0° (p,n) cross sections

General features of 0° ($q \sim 0$) (p,n) cross sections

J.Rapaport and E.Sugarbaker, Ann. Rev. Nucl. Part. Sci. 44, 109 (1994).

General features for light nuclei ($A=16-20$)

^{16}O : closed-shell, spin-saturated, $N=Z$

Fermi and GT states are not expected.

- Consistent with exp. data w/o peaks

Small c.s. is observed.

- Inclusion of np-nh configs. into the g.s.
→ Produce small GT strengths.

^{18}O : two extra neutrons in $d_{5/2}$

Strong GT transition by $n(d_{5/2}) \rightarrow p(d_{5/2})$ to $^{18}\text{F}(\text{g.s.})$

^{20}Ne : Deformed nuclei with $^{16}\text{O}+\alpha$ cluster

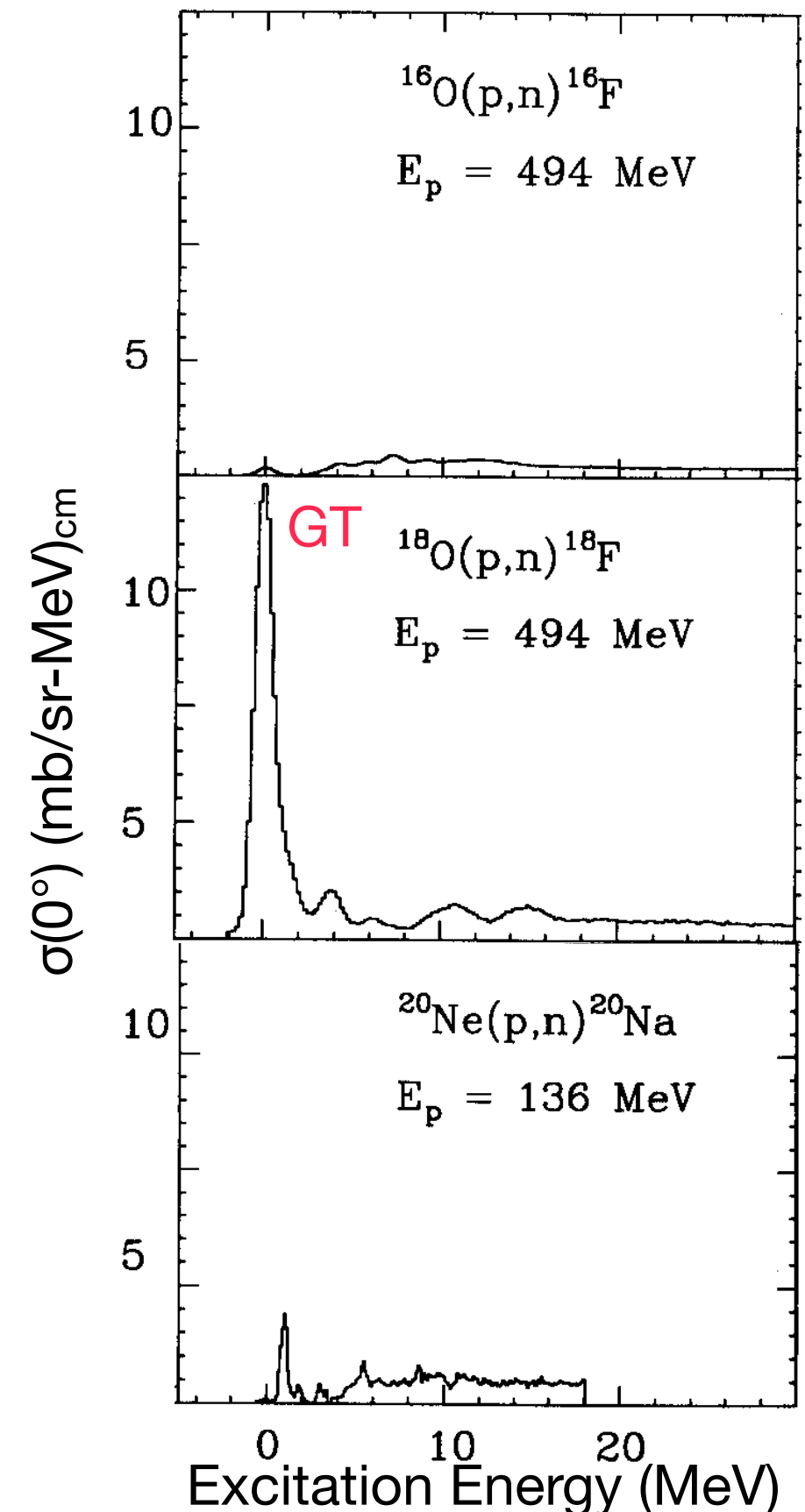
Spin-saturated config.

→ GT states are not expected.

- Consistent with exp. data w/o prominent peaks.

Small peaks are observed.

- Effects of np-nh configs. in the g.s.



General features of 0° ($q \sim 0$) (p,n) cross sections

J. Rapaport and E. Sugarbaker, Ann. Rev. Nucl. Part. Sci. 44, 109 (1994).

General features for medium and heavy nuclei

Medium mass nuclei of $A = 90-144$ ($N > Z$)

Sharp IAS (F) peaks are observed.

Roughly two GT bumps are observed.

- ^{90}Zr : $g_{9/2} \rightarrow g_{9/2}$ and $g_{9/2} \rightarrow g_{7/2}$ (main peak)

E_x of main GTR $>$ E_x of IAS

- IAS is between two GTR bumps

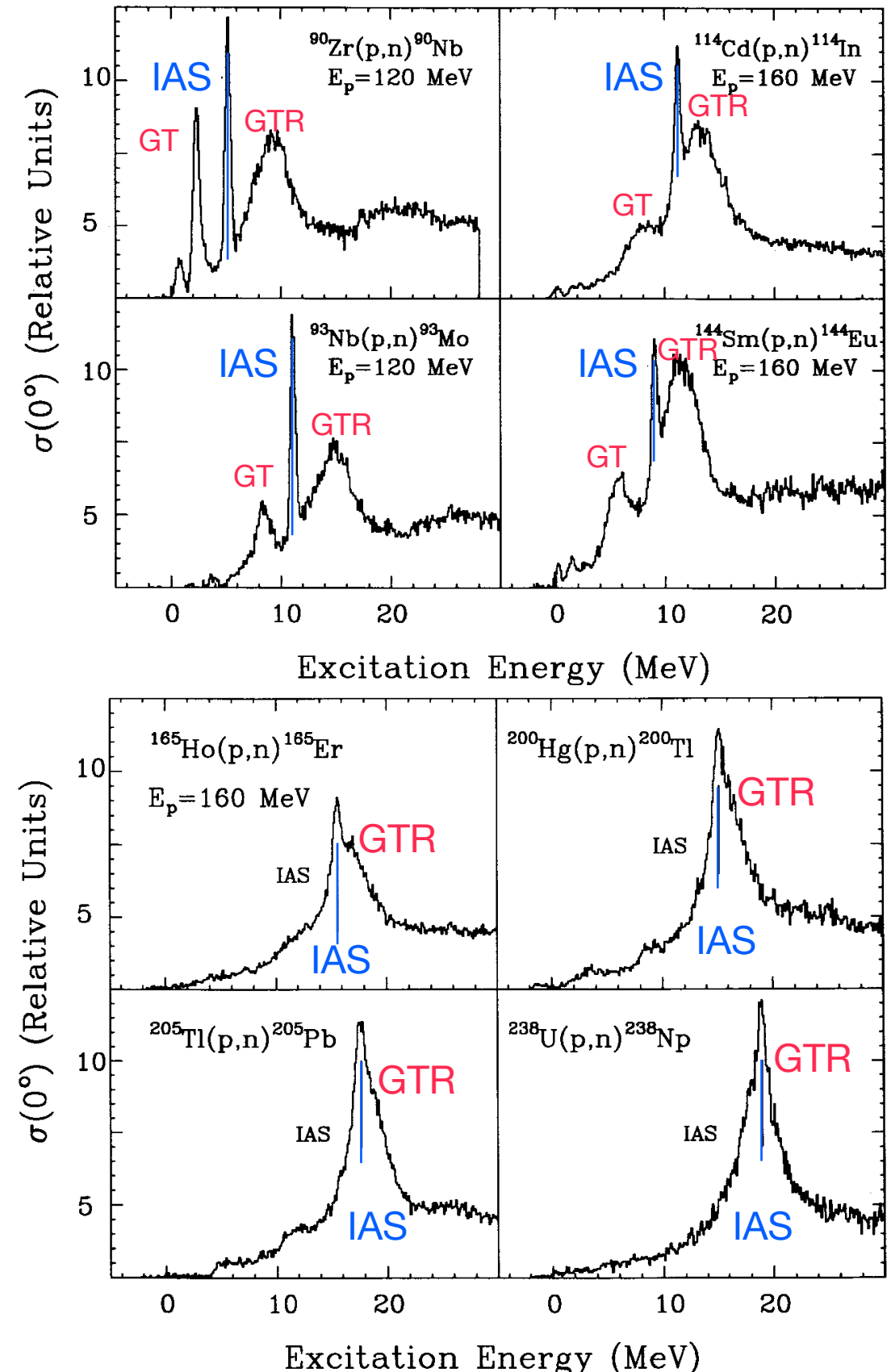
Heavy mass nuclei of $A \geq 165$

Peak positions of IAS and GTR are similar.

- IAS is NOT clearly observed with a moderate (p,n) resolution

One (high-energy) GTR bump is observed.

- Larger collectivity due to $N \gg Z$
- GT strengths concentrate to high GTR



Appendix B

Calibration method for
neutron detection efficiency

Intermediate energy neutron beams

Detection of fast neutrons with good energy resolutions:

- Accomplished with relatively small detector volume (for good timing resolution in TOF).
- Detection efficiency $\varepsilon < 100\%$

Efficiency ε should be determined to derive cross sections:

Monte-Carlo simulations by modeling nuclear reactions in detectors:

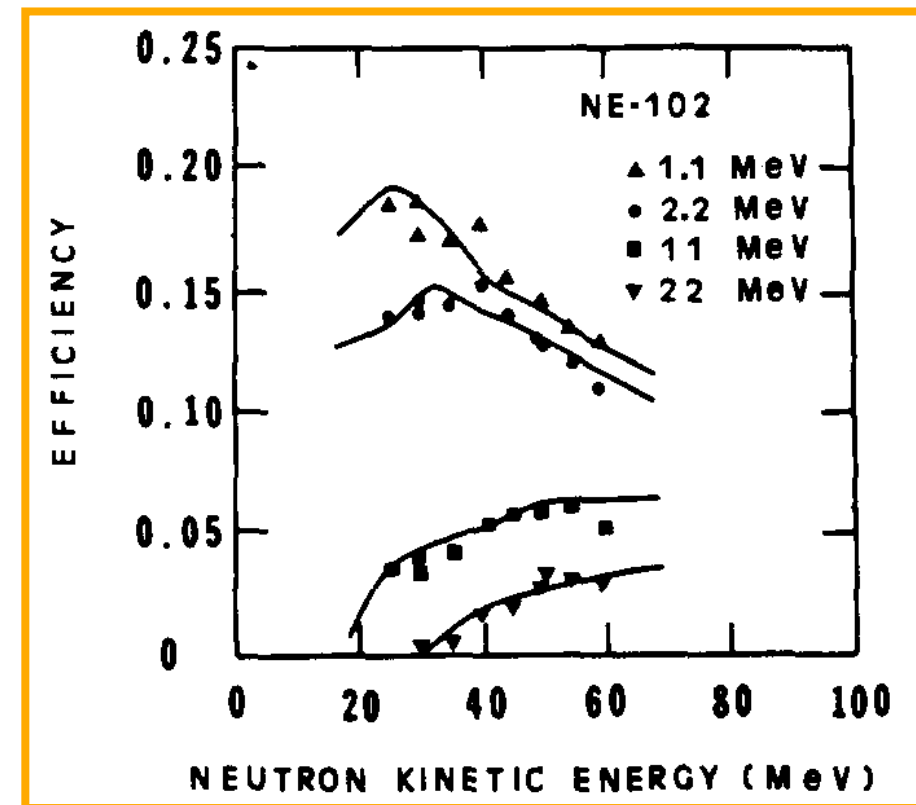
- agreement between exp. data and simulations $\sim 10\%$.
- Limited data for modeling at intermediate energies
→ Large uncertainty.

Tagged neutrons:

- Neutrons, n' , are produced by ${}^1\text{H}(n,n')p$
- Recoil protons, p , are measured.
 - Recoil proton flux = neutron flux (tagged).
- Efficiency ε can be calibrated with known neutron flux.

Use a neutron-production reaction with a known cross section.

- ${}^7\text{Li}(p,n){}^7\text{Be}(g.s.+0.43\text{ MeV})$ is commonly used.



*B.A.Cecil et al.,
Nucl. Instrum. Methods
161, 439 (1979).*

${}^7\text{Li}(p,n)$ as a neutron source w/ known flux

${}^7\text{Li}(p,n){}^7\text{Be}$

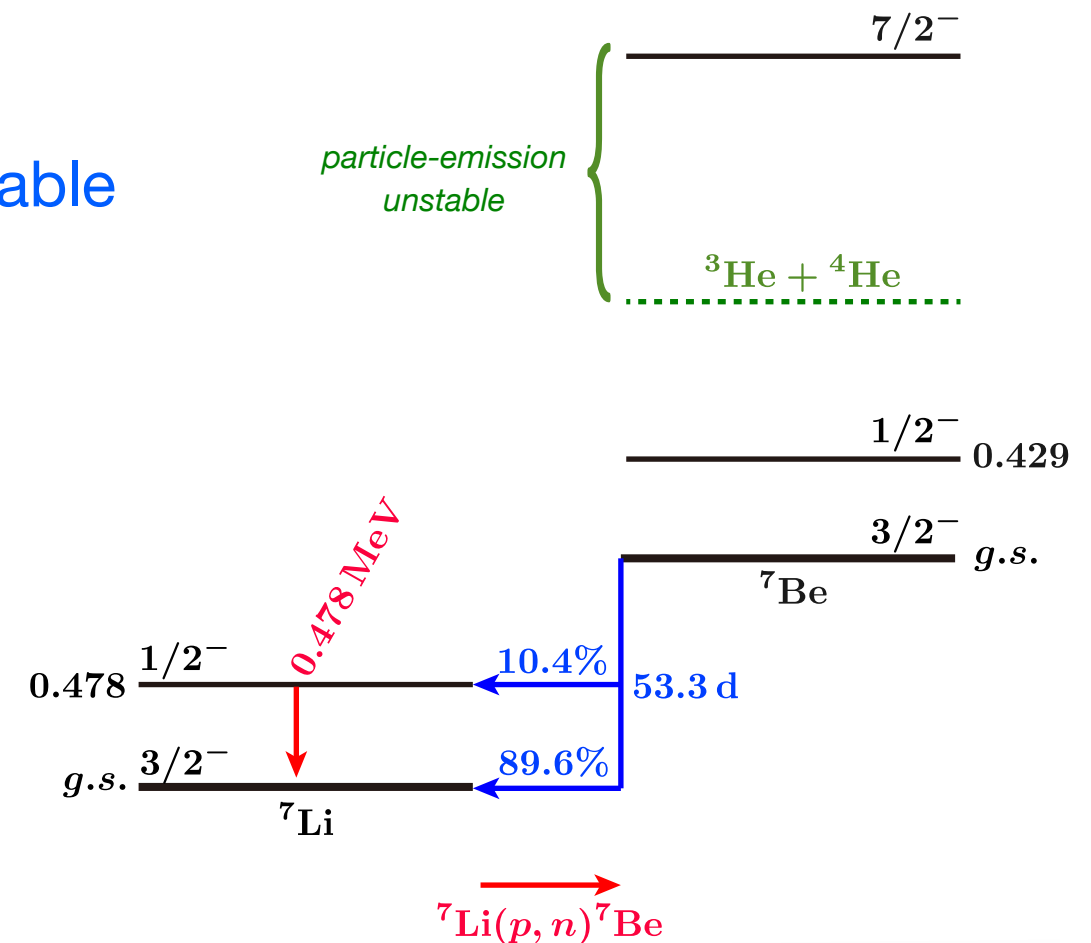
g.s. and 0.429 MeV of ${}^7\text{Be}$: **only particle-emission stable**

- Activation cross section for the production of ${}^7\text{Be}$
= Total cross section to these states

Half-life of ${}^7\text{Be}$ = 53.3d

→ 10.4% branching to ${}^7\text{Li}(0.478 \text{ MeV})$

- Total cross section, σ_T , can be measured
by measuring the 0.478 MeV γ -emission.

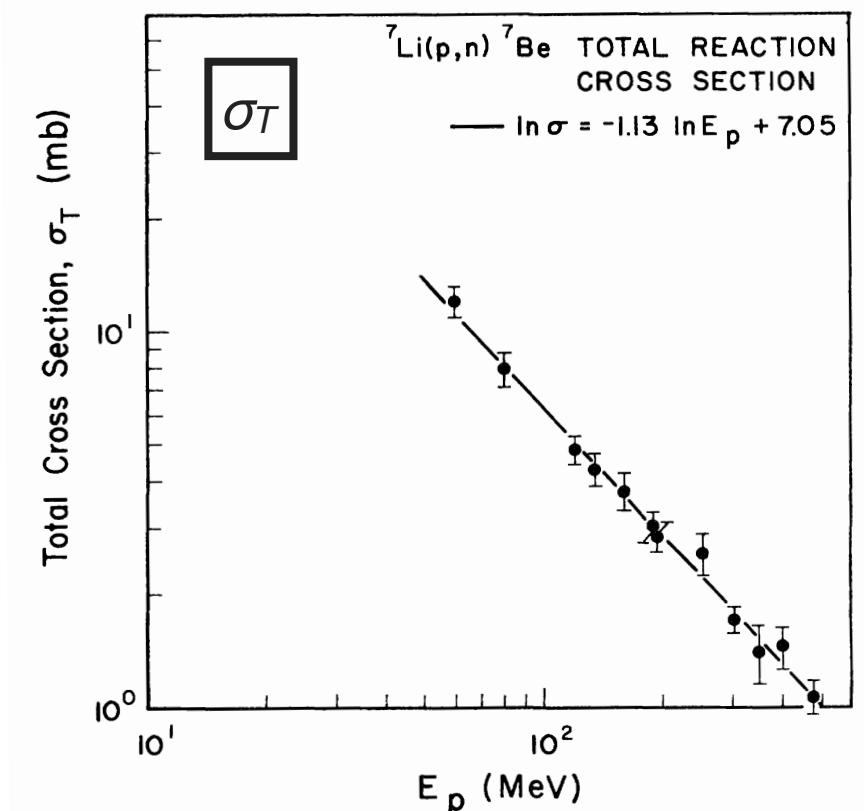


Experimental results for σ_T

$$\ln(\sigma_T)$$

$$= (7.02 \pm 0.05) + (-1.13 \pm 0.01) \ln(E_p)$$

- σ_T is well-known at $E_p = 25\text{-}480 \text{ MeV}$



L.Valentin, Nucl. Phys. 62, 81 (1965).

J.D'Auria et al., Phys. Rev. C 30, 1999(1984).

${}^7\text{Li}(p,n)$ as a neutron source w/ known flux

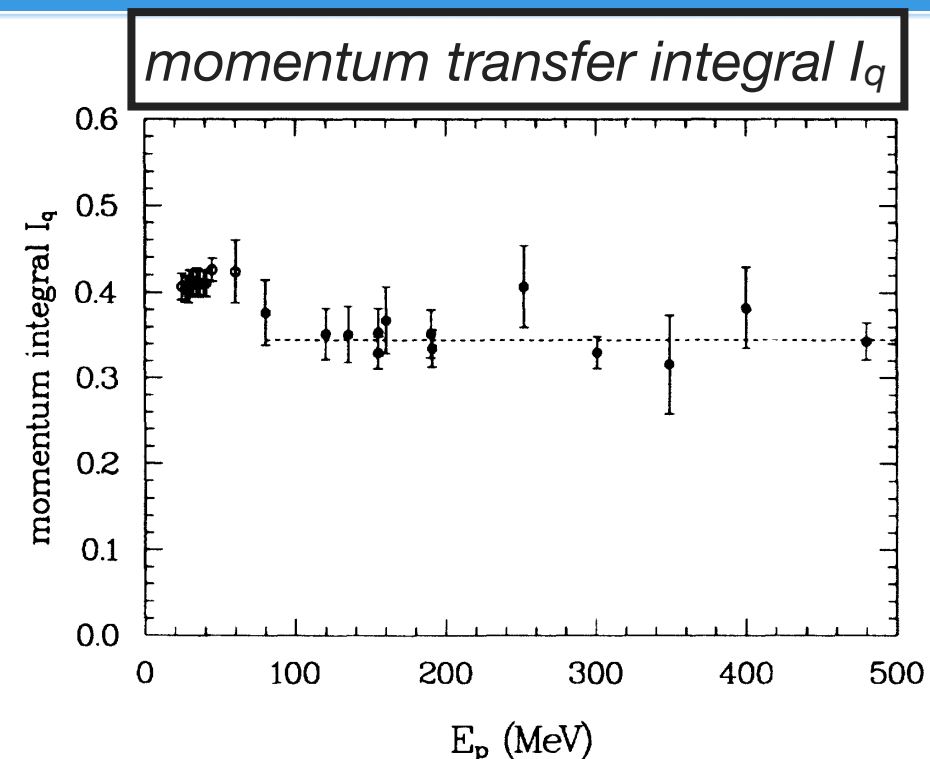
T.N. Taddeucci et al., Phys. Rev. C 41, 2548 (1990).

The total c.s., σ_T , is the integral of differential c.s. $\sigma(\theta)$:

$$\sigma_T = 2\pi \int_0^\pi \sigma(\theta) \sin \theta d\theta$$

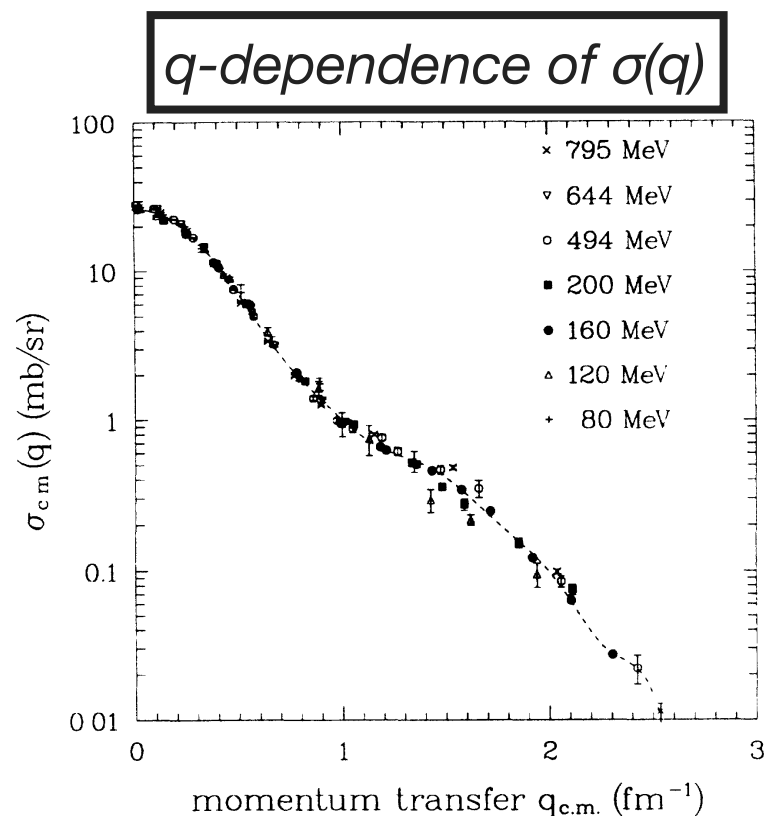
$$= \frac{2\pi}{k_i k_f} \int q\sigma(q) dq = \text{momentum-transfer integral : } I_q$$

- I_q deduced from σ_T are constant at $T_p \geq 80$ MeV.

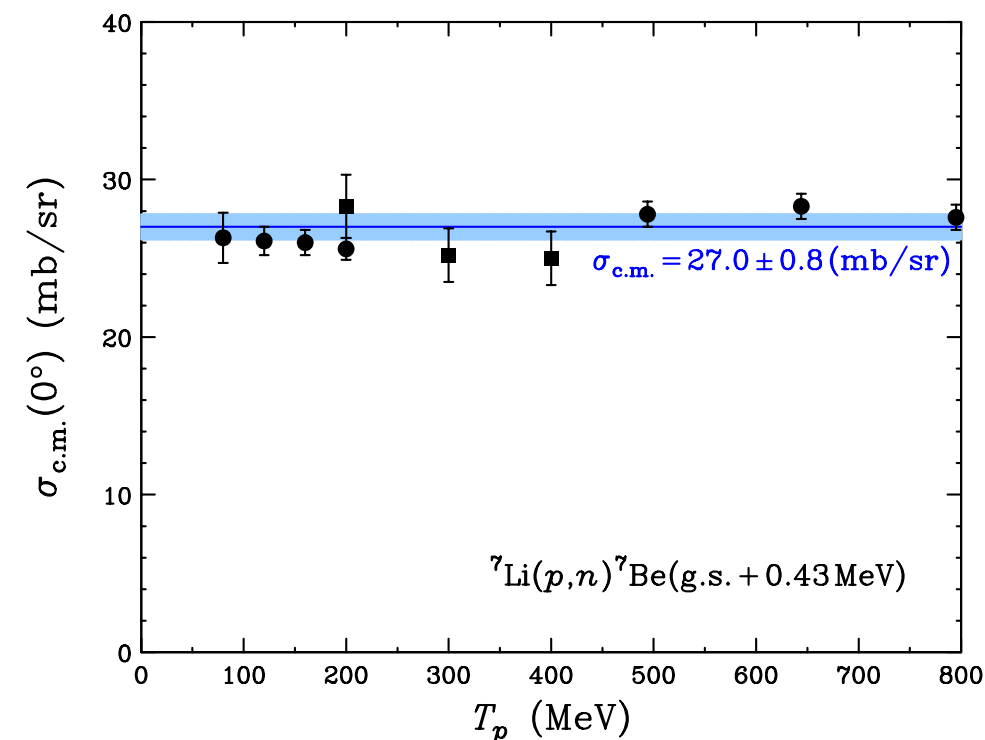


By measuring the relative q-dependence of $\sigma(q)$, absolute values can be deduced with:

$$\int q\sigma(q) dq = I_q = 0.345 \text{ (mb/sr)}$$



Final results for $\sigma_{c.m.}(0^\circ)$



c.m. cross sections are almost constant with 27.0 ± 0.8 mb/sr at $T_p = 80-795$ MeV

Appendix C

Theoretical predictions of SDR

Theoretical predictions for SD strengths

Spin-dipole operator:

$$\hat{O}_{SD}^J = (-1)^J \sum_{i=1}^A r_i [Y_1(\hat{r}_i) \otimes \vec{\sigma}_i]_{J\pi} t_{-,i}$$

Theoretical calculations

- 1st RPA : 1p-1h only
- 2nd RPA : 1p-1h + 2p-2h

Theoretical predictions:

SDR strength is spread out in $\omega=15-35$ MeV

Coupling to 2p-2h excitations causes:

- broadening of SDR distributions
- spreading to higher excitations

Sequence of SDR peak energies

- $2^- < 1^- < 0^-$
- same systematics of s.p. states.

